



Delft University of Technology

Wireless and Mobile Communication (WMC) Group
Department of Telecommunications
Faculty of Electrical Engineering, Mathematics and Computer Science
Delft University of Technology

Combining relaying and base station coordination for improving cell-edge multi-user performance in 3GPP LTE-Advanced networks

ASSIGNMENT : Master of Science Thesis
SUPERVISOR : Dr. Anthony Lo
DATE : June 14th, 2011
STUDENT : Peng Guan, 4039386

Combining relaying and base station coordination for improving cell-edge multi-user performance in 3GPP LTE-Advanced networks

THESIS

submitted in partial fulfillment of the
requirements for the degree of

MASTER OF SCIENCE

in

TELECOMMUNICATIONS

by

Peng Guan
born in Sichuan, P.R. China

This work was performed at:

Wireless and Mobile Communication (WMC) Group
Department of Telecommunications
Faculty of Electrical Engineering, Mathematics and Computer Science
Delft University of Technology

DELFT UNIVERSITY OF TECHNOLOGY

DEPARTMENT OF

TELECOMMUNICATIONS

The undersigned hereby certify that they have read and recommend to the Faculty of Electrical Engineering, Mathematics and Computer Science for acceptance a thesis entitled “**Combining relaying and base station coordination for improving cell-edge multi-user performance in 3GPP LTE-Advanced networks**” by **Peng Guan** in partial fulfillment of the requirements for the degree of **Master of Science**.

Date: June 14th, 2011

Committee Members

Responsible professor:

Prof.dr.ir. Ignas Niemegeers

Supervisor:

Dr.ir. Anthony Lo

Member:

Dr. Christian Doerr

Abstract

The emphasis of this thesis work is placed on improving cell-edge multi-user performance in 3GPP LTE-Advanced networks by utilizing relaying and base station coordination technologies. Relaying is a technology for enhancing the transmissions between two locations on a radio path and base station coordination is a multi-cell processing technology towards mitigating the inter-cell interference. In this report, we first study the capacity behavior of relaying. Two forward strategies: Amplify-and-forward (AF) and Decode-and-forward (DF), are modeled and compared. A new full duplex (FDX) operation mode of relaying is discussed, as well as a relay network with a multi-antenna receiver. Results show that FDX relaying outperforms half duplex (HDX) relaying, DF relaying has better performance than AF relaying under the condition of an ideal relay link (RL) and a multi-antenna receiver gains more from relaying than a single-antenna receiver. Then, we apply the pre-coding on the coordinated evolved Node B (eNB) to realize simultaneous multi-user transmissions on the same frequency band. The pre-coding matrix design is investigated and results show that zero-forcing (ZF) pre-coding of base station coordination reaches significant capacity enhancement in the case of a relatively high signal-to-noise-ratio (SNR). Finally, we propose a novel combination transmission scheme which integrates a shared relay node (RN) and coordinated eNBs in order to achieve higher multi-user sum-rate capacity. We show that the advantages of this combination scheme compared with applying each technology separately can be expected in most cases and it turns out to be a good improvement of the cell-edge multi-user performance.

Acknowledgements

This work was performed in the last year of my master study at Telecommunications department, Delft University of Technology. I would like to thank my supervisor Dr. Anthony Lo for his advice and support throughout the whole thesis work.

I would also like to thank all the lectures of Telecom department of TU Delft for enriching my knowledge in the area of communications.

Last but not least, I am indebted to all my friends and family for their love and encouragement.

Peng Guan
Delft, the Netherlands
June, 2011

Table of Contents

Abstract	I
Acknowledgements	III
Table of Contents	V
Notation	VII
Abbreviations	VIII
1 Introduction	1
1.1. Background	1
1.2. Problem statement	3
1.3. Organization of Thesis	5
2 Related work	6
2.1. LTE-Advanced architecture	7
2.2. Channel capacity	8
2.2.1. Mutual information	8
2.2.2. Gaussian channel capacity	8
2.3. Multi-input and multi-output	9
2.3.1. Single-user MIMO system model	9
2.3.2. MIMO Capacity	10
2.3.3. Multiplexing and diversity	11
2.3.4. MIMO MAC, MIMO BC and the duality	12
3 Relaying technology	15
3.1. The relay channel	15
3.2. Loop interference cancelling	16
3.3. Cooperative relaying	18
3.3.1. AF and DF	18
3.3.2. Half duplex relaying	18
3.3.3. Full duplex relaying	22
3.3.4. Numerical results	23
3.4. Multi-antenna receiver	26
4 Base station coordination	30
4.1. System model	30
4.2. Pre-coding in the downlink phase	31
4.3. Capacity improvement in the two-cell case	35
4.3.1. Conventional network	35
4.3.2. Base station coordination in the two-cell case	36
4.3.3. Numerical results	39
5 The combination	46

5.1.Shared relaying.....	46
5.2.System model	48
5.3.Performance evaluation	52
5.3.1.Four scenarios and simulation assumptions.....	52
5.3.2.Numerical results	54
6 Conclusion and future work.....	60
Appendices.....	62
Appendix A: WINNER II channel path loss models [124]	62
Reference.....	63
List of Figures.....	74
List of Tables	76

Notation

a	Scalar a (lowercase letter)
A	Set A (uppercase letter)
\mathbf{A}	Matrix \mathbf{A} (bold uppercase letter)
\mathbf{a}	Vector \mathbf{a} (bold lowercase letter)
\mathbf{A}^T	Transpose of matrix \mathbf{A}
\mathbf{A}^*	Conjugate transpose of matrix \mathbf{A}
\mathbf{A}^{-1}	Inverse of matrix \mathbf{A}
\mathbf{A}^+	Pseudo inverse of matrix \mathbf{A}
$\text{tr}(\mathbf{A})$	Trace of matrix \mathbf{A}
$\det(\mathbf{A})$	Determinant of matrix \mathbf{A}
$\dim(\mathbf{A})$	Dimension of matrix \mathbf{A}
$\ker(\mathbf{A})$	Null space of matrix \mathbf{A}
$\text{rank}(\mathbf{A})$	Rank of matrix \mathbf{A}
\mathbf{I}	Identity matrix
$\varepsilon\{\}$	Expectation operator
$\min\{x, y\}$	Minimum of x and y
$\max\{x, y\}$	Maximum of x and y
$\sup\{A\}$	Supremum of set A
$ z $	Modulus of complex number z
$\ \mathbf{a}\ $	Euclidean norm of vector \mathbf{a}
$(x)^+$	maximum of 0 and x
$\mathcal{CN}(\mu, \sigma^2)$	Complex Gaussian distribution with mean μ and variance σ^2
$\mathcal{N}(\mu, \sigma^2)$	Gaussian distribution with mean μ and variance σ^2

Abbreviations

3G	3rd Generation Mobile Telecommunications
3GPP	3rd Generation Partnership Project
4G	4th Generation Mobile Telecommunications
AF	Amplify-and-forward
AWGN	Additive white Gaussian noise
BC	Broadcast channel
BER	Bit-error rate
bps	Bits per second
CDMA	Code-division multiple access
CSI	Channel status information
CoMP	Coordinated multi-point transmission and reception
dB	Decibel
dBW	Decibel watt
DF	Decode-and-forward
DL	Downlink
DL	Direct link
DPC	Dirty paper coding
eNB	Evolved Node B
FDD	Frequency-division duplexing
FDX	Full-duplex
FDMA	Frequency-division multiple access
FER	Frame-error rate
GSM	Global System for Mobile Communications
HDX	Half-duplex
ITU	International Telecommunication Union
IMT	International Mobile Telecommunications
LOS	Line-of-sight
LTE	Long Term Evolution
NLOS	Non-line-of-sight
MAC	Multiple-access channel
MBSFN	Multi-Media Broadcast over a Single Frequency Network
MIMO	Multiple-input and multiple-output
MRC	Maximum ration combining
MU	Multi-user
MUD	Multi-user Detection
OFDM	Orthogonal frequency-division multiplexing
PSD	Positive semi-definite

RB	Resource block
RE	Resource element
RN	Relay node
SFN	Single Frequency Network
SNR	Signal-to-noise ratio
SINR	Signal-to-interference-and-noise ratio
STBC	Space-time block code
SVD	Singular-value decomposition
TDD	Time-division duplexing
TDMA	Time-division multiple access
UE	User equipment
UL	Uplink
UMTS	Universal Mobile Telecommunications System
WINNER	Wireless World Initiative New Radio model
WiMAX	Worldwide Interoperability for Microwave Access
ZF	Zero-forcing

1

INTRODUCTION

This chapter gives an introduction to the subjects we presented during the whole thesis work. Description of the background for this thesis work is in section 1.1 and the issues need to be addressed are presented in section 1.2. Finally there is a reading guide of the report in section 1.3.

1.1. Background

Cellular networks have been experiencing fast developments in recent years. After a great success of GSM and the communalization of 3G networks, International Telecommunication Union (ITU) proposed a new global standard framework ‘International Mobile Telecommunications (IMT) -Advance’ to build future generation cellular networks, which can fulfill the ever growing demands on capacities, motilities and so on. 3rd Generation Partnership Project (3GPP) Long Term Evolution (LTE) –Advanced [1] is one of candidates, even surpasses some requirements of IMT-Advanced, as shown in table 1.1.

Table 1.1. ITU and 3GPP requirements [116]

Quantity		IMT-Advanced	LTE-Advanced
Peak data rate	Uplink (UL)		1 Gbit/s
	Downlink (DL)		500 Mbit/s
Spectrum allocation		Up to 40 MHz	Up to 100 MHz
Latency	User plane	10 ms	10 ms
	Control plane	100 ms	50 ms
Spectrum efficiency (4 ant BS, 2 ant terminal)	Peak	15 bit/s/Hz DL	30 bit/s/Hz DL
		6.75 bit/s/Hz UL	15 bit/s/Hz UL
	Average	2.2 bit/s/Hz DL	2.6 bit/s/Hz DL
		1.4 bit/s/Hz UL	2.0 bit/s/Hz UL
	Cell-edge	0.06 bit/s/Hz DL	0.09 bit/s/Hz DL
0.03 bit/s/Hz UL		0.07 bit/s/Hz UL	

As shown in this table, not only the peak data rate and spectral efficiency, but also the cell-edge spectral efficiency is concerned in the requirements. The cell-edge spectral efficiency is actually a more important performance index in practice because ubiquitous high speed transmissions are expected in all the covered area of a modern cellular network.

In addition to the technique innovations in the early release of LTE, its evolution LTE-Advanced introduces more technology components for the purpose of improving system performance to fulfill IMT-Advanced requirements. And LTE-Advanced should be backwards compatible, which means it doesn't affect the existing LTE systems.

We can see in the table 1.1 that larger amounts of spectrum (up to 100 MHz) can be allocated for communications in LTE-Advanced networks. According to Shannon theory, the achievable channel capacity is linearly proportional to the bandwidth in the case of same SNR. Since the larger bandwidth results in higher capacity, LTE-Advanced introduces carrier aggregation[1] to allocate such a large bandwidth in a non-contiguous way to enhance the system performance.

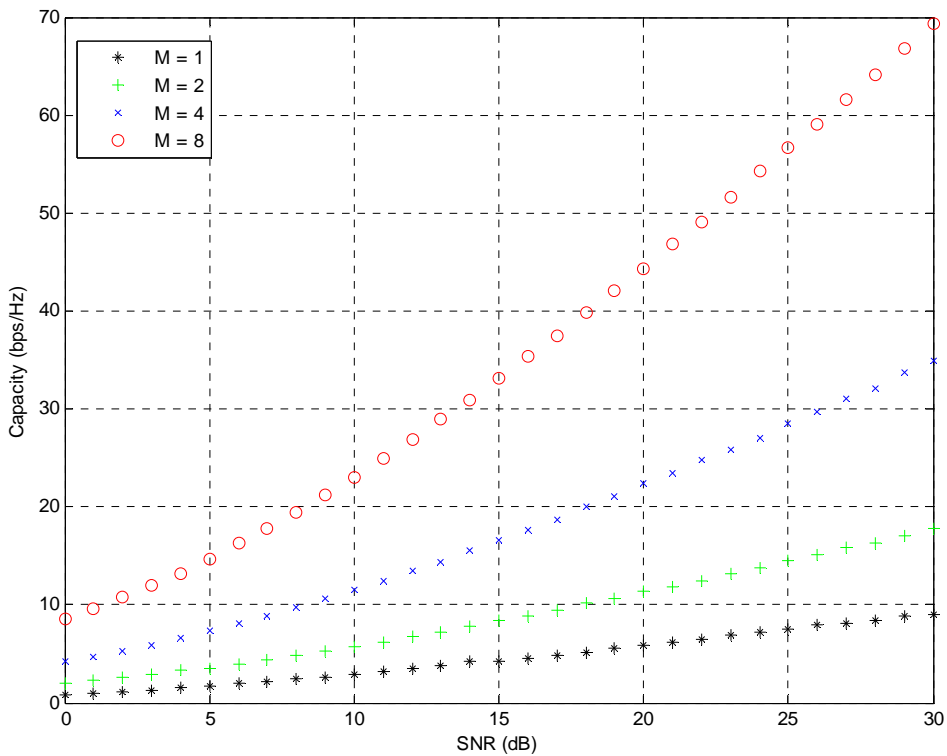


Figure 1.1. Capacity versus SNR for different antenna configurations: M = 1, 2, 4 and 8

Multiple-input multiple-output (MIMO) technology is an efficient transmission scheme which significantly improves the system performance by exploiting the multi-path scattering. LTE-Advanced adapts enhanced multi-antenna transmission for the higher capacity. It is suggested that 8×8 antenna configuration[1] (i.e., 8 transmit antennas and 8 receive antennas) can be used in the LTE-Advanced networks. Figure 1.1 shows the benefit in capacity we can get from the MIMO technology in four different configurations with M transmit antennas \times M receive antennas, $M = 1, 2, 4, 8$, respectively. We can see in this figure that with the increase in the number of antennas, the achievable capacity of the MIMO system increases considerably.

1.2.Problem statement

The long lasting problem on wireless system design is how to achieve a higher system capacity with lower resource consumptions. The term “resource” here is used to refer to time, frequency and power which can be allocated by the network operators.

Specifically, in the cellular networks, we always face a challenging problem that the performance of cell-edge users is much worse than the users in the cell center.

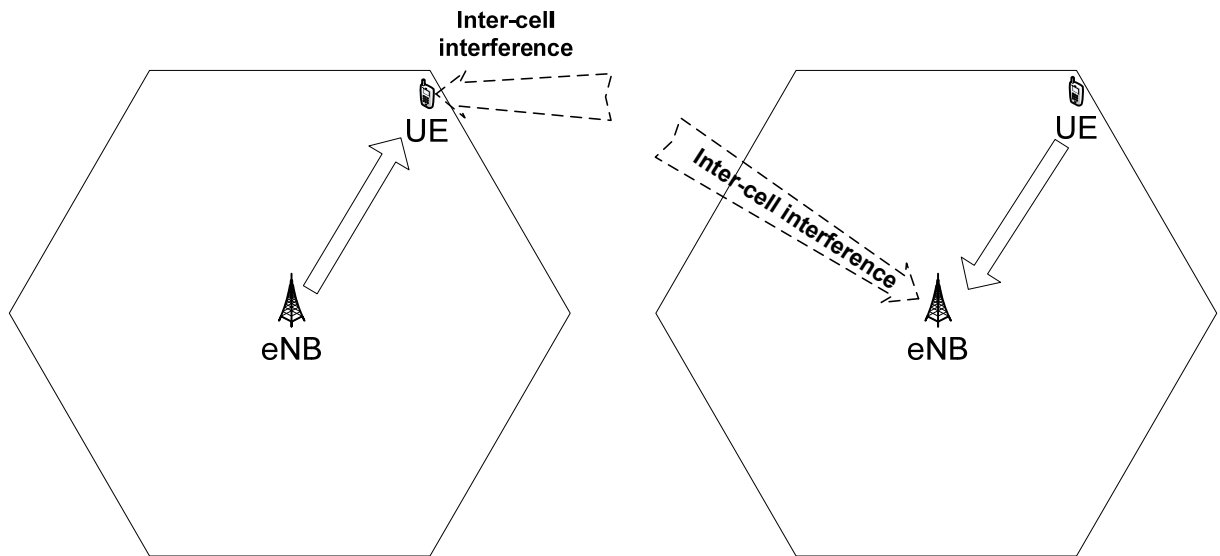


Figure 1.2. Illustrations of inter-cell interference: downlink phase (left) and uplink phase (right), where the solid arrow denotes the transmission of useful signal and the dashed arrow denotes the inter-cell interference

The first reason of the performance degradation of the cell-edge users is the long distance

between the eNB and the UE and the limited power of the transmit antennas. It is known that the signal strength decreases proportionally to the exponentiation of the distance in the wireless communications. With the limited power of transmit antennas, the receiver would get very weak useful signal in a noisy environment, and the low receive SNR results in a low data rate.

The second reason is the inter-cell interference. In both uplink and downlink phases, transmissions in one cell would interfere the transmissions in the other neighbor cells if they are operated on the same resource. As shown in figure 1.2, in the downlink, the UE on the cell board is interfered by the signals from other cells (denoted by a dashed arrow) so that it could not successfully recover the signal for its associated eNB (denoted by a solid arrow); in the uplink, the eNB is interfered by the signals from other cells (denoted by a dashed arrow) so that it could not successfully recover the signal transmitted by the UE (denoted by a solid arrow).

According to the discussions above, if we want to improve the cell edge performance, we should find an efficient solution to the two problems:

1. How to enhance the wireless links;
2. How to cancel the inter-cell interference.

The past experience tells us that relaying is a cost-efficient solution for the coverage holes in the cellular network and we can use this technology to enhance the wireless links between the transmitter and receiver. The relay node can physically reduce the distance between the transmitter and receiver and therefore lead to a higher receive SNR at the receiver. LTE-Advanced also includes advanced relaying[1] in its technique specifications. With the relay deployment in the network, we can realize cooperative transmissions between the relay and the transmitter, which will be discussed in Chapter 3 in details.

The straightforward method of addressing the inter-cell interference is avoiding it by assigning orthogonal resources to different cells, such as reusing the frequency bands or transmitting in different time slots. LTE-Advanced proposes coordinated multi-point transmission and reception (CoMP)[1] for this kind of dynamic scheduling. Considering the preciousness of these resources, it is a better idea to work towards developing a new transmission scheme which could allow multi-user transmissions on the same resource to increase the utilization efficiency. We use the term “base station coordination” to denote this kind of joint multi-cell multi-user transmission scheme.

Thank to the feasibility of tight coordinations between the eNBs in LTE-Advanced networks, multi-user multiple-input multiple-output (MU-MIMO) technology can be applied. We can coordinate the transmit antennas of different eNBs in different cells to

CHAPTER 1 INTRODUCTION

form a virtual transmit antenna array and then the simultaneous transmissions to different users on the same frequency band form a MIMO broadcast channel, for which the more detailed analysis is in Chapter 4.

Enhancing the wireless links by relaying and mitigating the inter-cell interference by base station coordination can be done concurrently. The thesis work shows the practicability and advantages of this combined scheme and it turns out to be a good solution to the two problems we proposed before.

1.3. Organization of Thesis

The thesis work adds new content to two enhanced technology components in LTE-Advanced networks: relaying and base station coordination, and combines them in a more efficient transmission scheme for cell-edge users. The methodologies and system models are described, the performance is evaluated as well.

In the following parts of this thesis report, Chapter 2 provides an overview of related work and current research status. Chapter 3 analyzes the relaying behaviors with different configurations and realizes full duplex relaying. Chapter 4 addresses multi-cell multi-user transmissions through base station coordination and estimates the numerical results. Chapter 5 proposes a hybrid scheme of the two components mentioned above and the sum-rate capacity is compared with those in conventional networks and the networks applying each technology separately. The report ends with an conclusion and suggestions for future research.

2

RELATED WORK

Both the 3GPP and IEEE workgroups submitted their proposals to ITU for candidate radio interface technologies for the IMT-Advanced: LTE-Advanced [1] and 802.16e [2][3] respectively. [73][99][114][116] provided overviews of features and components in LTE and its later evolution LTE-Advanced. [2][124] modeled the typical channels which can be used for estimating and simulating cellular networks in different radio environments.

There is a common agreement that OFDMA will replace CDMA to be the fundamental radio technology in the 4G cellular networks, and MIMO technology is integrated in the transmission scheme with OFDMA. [9][26][27][30][78][79][91] discussed the design and limits of a MIMO system in various aspects, especially in the achievable capacity of the multiple antenna system.

LTE and its evolution can support channel-dependent scheduling in both the time and frequency domain. [11][37][53][70][84][102] developed scheduling algorithms to exploit the channel variations to realize efficient utilization of the available radio resources.

Relaying has been studied since early 70's last century and a lot of achievements are available today. [3][6][40][109][111][128] suggested different relay architectures. [15][31][45][60] investigated the information-theoretical capacity bound for a relay channel, under different channel model assumptions. [4][95] indicated the feasibility of cancelling the loop interference on the relay station. [17][110] developed resource allocation algorithms for a relay system.

The multi-user information theory has received growing attentions in recent years. With multi-cell processing, it is a promising method to deal with the inter-cell interference in a cellular network like LTE-Advanced. [47][65] proposed the different multi-user transmission schemes, [112][115] studied the achievable capacity region of the multiple users, [5][94][113][122][123] looked into the uplink-downlink duality theory, [13][14][49][51][119][126] aimed to solve the problems in the pre-coding design.

[32][33][34][117][121] also proposed a system integrating relaying and coordinated base stations.

In the following part of this chapter, some essential theories, formulas and models for the whole thesis work are explained in details. Section 2.1 reviews the architecture of LTE-Advanced networks. Section 2.2 introduces the concepts and estimation methods of channel capacity. Section 2.3 gives holistic descriptions of MIMO systems.

2.1.LTE-Advanced architecture

The network architecture of LTE-Advanced Multihop Cellular Networks (MCN) is shown in Figure 2.1[128]. The MCN is composed of one or more relays between an eNB and a UE. A single eNB serves one or more multi-hop chains in its cell, which forms a tree structure. The number of relays in a multi-hop chain is $n - 1$ for n number of hops. The complexity is related to the number of hops. Thus, 3GPP has limited n to two for LTE-Advanced MCN.

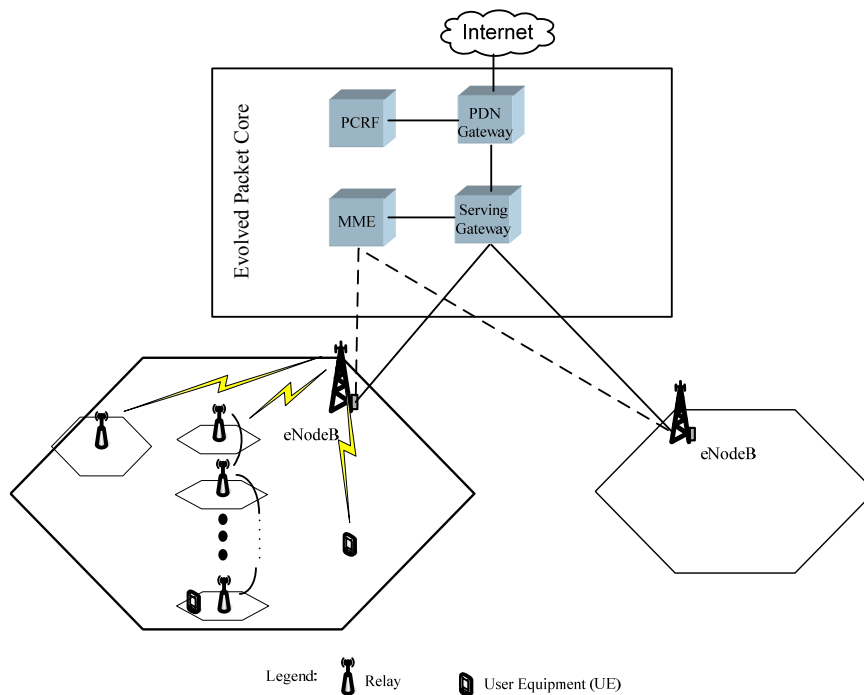


Figure 2.1.LTE-Advanced Multi-hop Cellular Network Architecture [128]

[73] As to the resource management in LTE-like networks, the smallest unit in the resource grid is the resource element (RE), which is associated with one subcarrier frequency band during one symbol duration. The spacing of OFDM subcarriers in the frequency domain is 15 kHz. 7 such symbol durations form one time slot (0.5 ms) and 12 subcarriers (180 KHz) during one time slot form one resource block (RB). The smallest

amount of resource that can be assigned by the scheduler is two RBs.

LTE-like networks support both Time Division Duplex (TDD) and Frequency Division Duplex (FDD) operations so that the uplink and downlink transmissions can be considered as independent processes.

2.2.Channel capacity

Capacity is the most important performance indicator of a communication system. This section reviews the estimation of channel capacity.

2.2.1.Mutual information

Shannon showed that the channel capacity is equal to the mutual information, maximized over all input distributions, [57] i.e.

$$C = \max_{p(x)} I(X; Y), \quad (2.1)$$

where $p(x)$ is the marginal probability density function of the random input variable.

The mutual information between random input X and random output Y over a communication channel is [57]

$$I(X; Y) = \int_Y \int_X p(x, y) \log_2 \left(\frac{p(x, y)}{p(x)p(y)} \right) dx dy, \quad (2.2)$$

where $p(y)$ is the marginal probability density function of the random output variable and $p(x, y)$ is the joint probability density function.

2.2.2.Gaussian channel capacity

For a Gaussian channel, the channel capacity is [125]

$$C = \frac{1}{2} \log_2(1 + \gamma) \text{ bits per transmission}, \quad (2.3)$$

where γ denotes the signal-to-noise-ratio (SNR) of the wireless link.

Shannon-Hartley theorem pointed out that the capacity of a limited bandwidth Gaussian channel is [125]

$$C = B \log_2(1 + \gamma) \text{ bits per second}, \quad (2.4)$$

where B denotes the bandwidth.

The interference in a network can also be modeled as Gaussian due to the central limit theorem, then the capacity of an interfered channel can be determined by

$$C = B \log_2(1 + SINR) \text{ bits per second,} \quad (2.5)$$

where $SINR$ denotes the signal-to-interference-and-noise-ratio.

Typically, considering radio propagations in reality, one of the applicable wireless channel models is Rayleigh fading. The Rayleigh fading channel can be represented by a complex number, the real and imaginary parts of which are independent and identically distributed (i.i.d.) zero-mean Gaussian processes. For example, an ideal Rayleigh fading channel is $Z = X + jY \sim$ i.i.d. complex Gaussian distributed $\mathcal{CN}(0,1)$ if X and Y are \sim i.i.d. Gaussian distributed $\mathcal{N}(0,1/2)$. This complex Gaussian assumption of a Rayleigh fading channel is utilized in all the numerical evaluations and simulations in this report.

2.3. Multi-input and multi-output

MIMO technology could significantly enhance the wireless system performance by reusing the space dimensions and exploiting multi-path scattering.

2.3.1. Single-user MIMO system model

[9][26] For a system with M_T transmit antennas and M_R receive antennas, the MIMO channel can be expressed by a $M_R \times M_T$ matrix

$$\mathbf{H} = \begin{pmatrix} h_{1,1} & h_{2,1} & \cdots & h_{M_T,1} \\ h_{1,2} & h_{2,2} & \cdots & h_{M_T,2} \\ \vdots & \vdots & \ddots & \vdots \\ h_{1,M_R} & h_{2,M_R} & \cdots & h_{M_T,M_R} \end{pmatrix}, \quad (2.6)$$

where $h_{m,n}$ denotes the channel gain between m th transmit antenna and n th receive antenna. The receiver observes

$$\mathbf{y} = \mathbf{H}\mathbf{x} + \mathbf{n}, \quad (2.7)$$

where the $M_R \times 1$ vector $\mathbf{y} = \begin{pmatrix} y_1 \\ y_2 \\ \vdots \\ y_{M_R} \end{pmatrix}$, $M_T \times 1$ vector $\mathbf{x} = \begin{pmatrix} x_1 \\ x_2 \\ \vdots \\ x_{M_T} \end{pmatrix}$ and $M_R \times 1$ vector

$\mathbf{n} = \begin{pmatrix} n_1 \\ n_2 \\ \vdots \\ n_{M_R} \end{pmatrix}$ denote the receive signals, transmit signals and noises, respectively. In a

single-user system, the total power of the transmit antennas is limited as P , i.e. $\mathcal{E}\{\mathbf{x}^* \mathbf{x}\} \leq P$. The noises are assumed to be additive white circularly symmetric complex

Gaussian, which can be normalized to unity, i.e. $\mathcal{E}\{\mathbf{nn}^*\} = \mathbf{I}_{M_R}$, so that P is also the expression of the *SNR* of the MIMO channel.

2.3.2.MIMO Capacity

[79] In a MIMO system, if the channel matrix is constant and perfectly known on both of the transmit and receive sides, the channel capacity can be calculated by

$$C = \max_{\mathbf{Q}: \text{tr}(\mathbf{Q})=P} \log_2 \det(\mathbf{I}_{M_R} + \mathbf{H}\mathbf{Q}\mathbf{H}^*), \quad (2.8)$$

where the $M_T \times M_T$ covariance matrix \mathbf{Q} of the input variables is positive semi-definite.

[23] In a tangible wireless communication system, the channel is time variant. Considering the slow flat fading channel, which is the case in LTE-like cellular networks when OFDM technology is applied, the ergodic MIMO capacity is the average of capacities in each channel realization

$$C = \mathcal{E}_{\mathbf{H}} \left\{ \max_{\mathbf{Q}: \text{tr}(\mathbf{Q})=P} \log_2 \det(\mathbf{I}_{M_R} + \mathbf{H}\mathbf{Q}\mathbf{H}^*) \right\}, \quad (2.9)$$

in which the channel matrix \mathbf{H} and input covariance \mathbf{Q} are time-dependent.

[118] Rewrite \mathbf{H} with singular value decomposition (SVD) as

$$\mathbf{H} = \mathbf{U}\mathbf{\Sigma}\mathbf{V}^*, \quad (2.10)$$

where \mathbf{U} is a $M_R \times M_R$ unitary matrix, \mathbf{V}^* is a $M_T \times M_T$ unitary matrix and $\mathbf{\Sigma}$ is a $M_T \times M_R$ diagonal matrix with nonnegative real numbers Σ_i for the diagonal elements, which are in fact the singular values of \mathbf{H} . Note that the rank of \mathbf{H} $R_{\mathbf{H}} = \text{rank}(\mathbf{H}) \leq \min(M_T, M_R)$. So the number of the non-zero diagonal elements in $\mathbf{\Sigma}$ is $R_{\mathbf{H}}$.

[79] The wireless channel could be treated as $R_{\mathbf{H}}$ parallel channels when appropriate pre- and post- proceedings for the input and output are applied. Construct \mathbf{x} with a pre-coding matrix \mathbf{V} ,

$$\mathbf{x} = \mathbf{V}\mathbf{d}, \quad (2.11)$$

where \mathbf{d} is the data symbol vector. Decode \mathbf{y} at the receiver by \mathbf{U}^* to get

$$\tilde{\mathbf{y}} = \mathbf{U}^* \mathbf{y} = \mathbf{U}^* (\mathbf{U} \mathbf{\Sigma} \mathbf{V}^* (\mathbf{V} \mathbf{d}) + \mathbf{n}) = \mathbf{\Sigma} \mathbf{d} + \tilde{\mathbf{n}}, \quad (2.12)$$

where $\tilde{\mathbf{n}} = \mathbf{U}^* \mathbf{n}$ is the noise vector which has the same distribution as \mathbf{n} because of the unitarity of \mathbf{U}^* .

[79] For each of the parallel channel, the signal power is set as P_i , and assume the water-filling level is ν , then the individual power of each transmit signal should satisfy the condition

$$P_i = \left(\nu - \frac{1}{\Sigma_i^2} \right)^+ \quad (2.13)$$

to achieve the maximum total allowed power $P = \sum_{i=1}^{R_H} P_i$, where $(x)^+$ denotes $\max(0, x)$. This water-filling power allocation algorithm results in a capacity

$$C = \sum_{i=1}^{R_H} \left(\log_2 \left(\nu \Sigma_i^2 \right) \right)^+ . \quad (2.14)$$

To achieve the capacity in (2.14), the covariance matrix \mathbf{Q} in (2.8) is $\mathbf{Q} = \mathbf{V} \mathbf{P} \mathbf{V}^*$, where the matrix \mathbf{P} is a diagonal matrix that $\mathbf{P} = \text{diag}(P_1, \dots, P_{R_H}, 0, \dots, 0)$.

[24] In a slow flat fading channel, there is a possibility p that the errors occur when the transmitter transmits at the rate $C_{out,p}(P)$, i.e.

$$P_e(P, C_{out,p}(P)) = p\%, \quad (2.15)$$

where p is called outage probability and $C_{out,p}(P)$ is the outage capacity, with a certain SNR (or P if consider unit noise power).

2.3.3. Multiplexing and diversity

In a communication system, multiplexing [44][50][79] is commonly used for improving the capacity and diversity [42][50][79] is the important technology for combating fading, noise and interference. The maximum multiplexing gain of a MIMO system at a given outage probability p is

$$\lim_{P \rightarrow \infty} \frac{C_{out,p}(P)}{\log_2 P}, \quad (2.16)$$

and the maximum diversity gain of a MIMO system at a given transmission rate R is

$$-\lim_{P \rightarrow \infty} \frac{\log_2 P_e(P, R)}{\log_2 P}. \quad (2.17)$$

With optimal design of the transmitter and receiver, the achievable maximum multiplexing gain and diversity gain [79] are $\min\{M_R, M_T\}$ and $M_R M_T$, respectively. For a MIMO system, with the increased SNR , multiplexing means increasing the transmission rate at a fixed error rate and diversity means reducing the error rate at a fixed transmission rate. The decision of whether utilizing the increased SNR in multiplexing or diversity forms an important trade-off problem in MIMO transmissions.

When each the transmit antenna transmits independent signals, the space dimensions are reused, which is called spatial multiplexing. [93] The maximum order of spatial multiplexing in a MIMO system is $\min\{M_R, M_T\}$, but limited by the spatial correlation in a practical environment.

For simplicity, the channel matrix \mathbf{H} should be equal to \mathbf{H}_w , in which the matrix elements are independent and identically distributed circular symmetric complex Gaussian with zero-mean and unit variance ($\sim \mathcal{CN}(0,1)$). However, correlations of the transmit antennas and correlations of the receive antennas have to be taken into considerations. [79][93] Spatial correlation matrixes \mathbf{R}_T and \mathbf{R}_R are used in Kronecker model for factorizing the channel matrix

$$\mathbf{H} = \mathbf{R}_R^{1/2} \mathbf{H}_w (\mathbf{R}_T^{1/2})^T. \quad (2.18)$$

It is suggested [9] that when the distance between separated antennas is larger than half of the signal wavelength the spatial correlation can be ignored and \mathbf{R}_T and \mathbf{R}_R are then identity matrices.

2.3.4. MIMO MAC, MIMO BC and the duality

A multiple access channel (MAC) is a channel with one receiver and multiple transmitters and on the contrary a broadcast channel (BC) is a channel with one transmitter and multiple receivers. It is known that the channel capacity for multi-user transmissions is a region instead of a real-number value and the duality of the MAC and BC exists in the single-antenna network. [57] It would also be a big advantage of a MIMO system if it can support the communications of the various users simultaneously on the same frequency band.

As shown in figure 2.2, on the left side, one transmitter with M_T transmit antennas broadcasts to K receivers each with M_R receive antennas, which forms a MIMO BC; on the right side, K transmitters each with M_R transmit antennas access one receiver with M_T receive antennas, which forms a MIMO MAC. In a LTE-Advanced network, we can use

MIMO MAC to represent the uplink transmissions from K UEs to the eNB and MIMO BC to represent downlink transmissions from the eNB to K UEs. With the duality assumption, the channel gains in the uplink phase are considered as conjugate transposes of the corresponding channel gains in the downlink phase. [79]

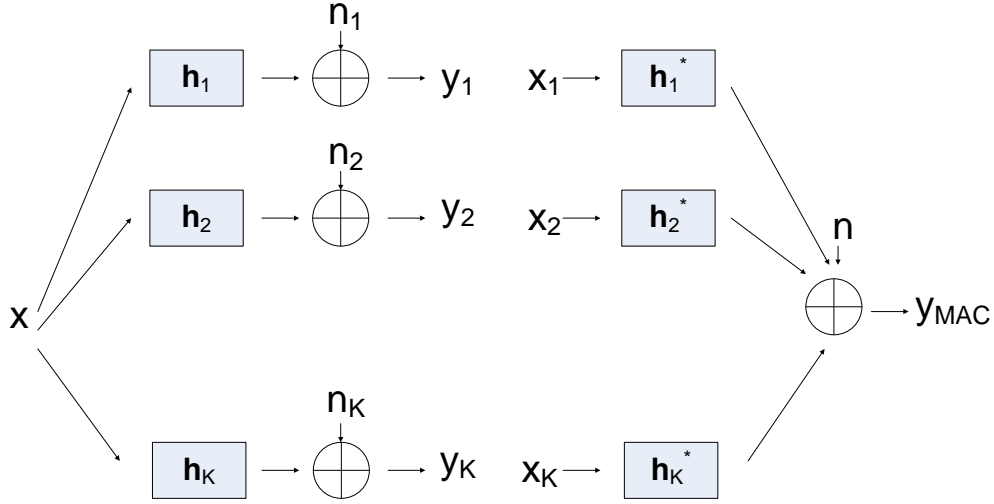


Figure 2.2.MIMO BC (left) and MIMO MAC (right)

The MIMO MAC can be modeled as

$$\mathbf{y}_{MAC} = \sum_{k=1}^K \mathbf{h}_k^* \mathbf{x}_k + \mathbf{n}, \quad (2.19)$$

where $M_T \times 1$ vector \mathbf{y}_{MAC} is the receive signal vector at the eNB, $M_R \times 1$ vector \mathbf{x}_k is the transmit signal vector from the k th UE, $M_T \times M_R$ matrix \mathbf{h}_k^* is the corresponding channel from k th UE to the eNB and $M_T \times 1$ vector \mathbf{n} is noise vector observed at the eNB.

And the MIMO BC can be modeled as

$$\mathbf{y}_k = \mathbf{h}_k \mathbf{x} + \mathbf{n}_k, \quad (2.20)$$

where $M_R \times 1$ vector \mathbf{y}_k is the receive signal vector at k th UE, $M_T \times 1$ vector \mathbf{x} is the transmit signal vector from the eNB, $M_R \times M_T$ matrix \mathbf{h}_k is the corresponding channel from the eNB to the k th UE and $M_R \times 1$ vector \mathbf{n}_k is noise vector observed at the k th UE.

[79][94] indicated that the uplink-downlink duality also holds for the capacities of MIMO MAC and MIMO BC. The capacity region has an expression as

$$\begin{aligned}
 C_{BC}(P; \mathbf{H}) &= C_{MAC}(P; \mathbf{H}^*) \\
 &= \bigcup_{\left\{ \mathbf{Q}_i \geq 0, \sum_{i=1}^K \text{tr}(\mathbf{Q}_i) \leq P \right\}} \left\{ (R_1, \dots, R_K) : \sum_{i \in S} R_i \leq \log_2 \det \left(\mathbf{I}_{M_T} + \sum_{i \in S} \mathbf{h}_i^* \mathbf{Q}_i \mathbf{h}_i \right) \forall S \subseteq \{1, \dots, K\} \right\}, \quad (2.21)
 \end{aligned}$$

where \mathbf{H} is the BC matrix and its conjugate transpose \mathbf{H}^* is the MAC matrix, P is the total power allowed at the transmit antennas, \mathbf{Q}_i is the covariance matrix of i th input, R_i is the achievable rate for i th user and S is the subset of $\{1, \dots, K\}$.

3

RELAYING TECHNOLOGY

The very high data rates target, particularly for users on the cell board, is a challenging problem for the LTE-Advanced networks, which motivates the deployment of the denser infrastructure. Multi-hop relay [3][6][86] is considered as one cost-efficient solution to improve the coverage and capacity of cellular networks. [28] Generally, in a 3GPP LTE cellular network, the number of hops is limited as two, and the relay stations are assumed to be fixed, which means the nomadic relays [88][108] are not in the consideration of this report.

Section 3.1 recalls the cut-set upper bound for the relay channel. Section 3.2 introduces loop interference cancelling technology. Section 3.3 analyzes the cooperative transmissions between the eNB and the RN. Section 3.4 extends the analysis to a relay network with multi-antenna UEs.

3.1. The relay channel

A basic relay system consists of three nodes, the source (S), the relay (RN) and the destination (D), as shown in figure 3.1.

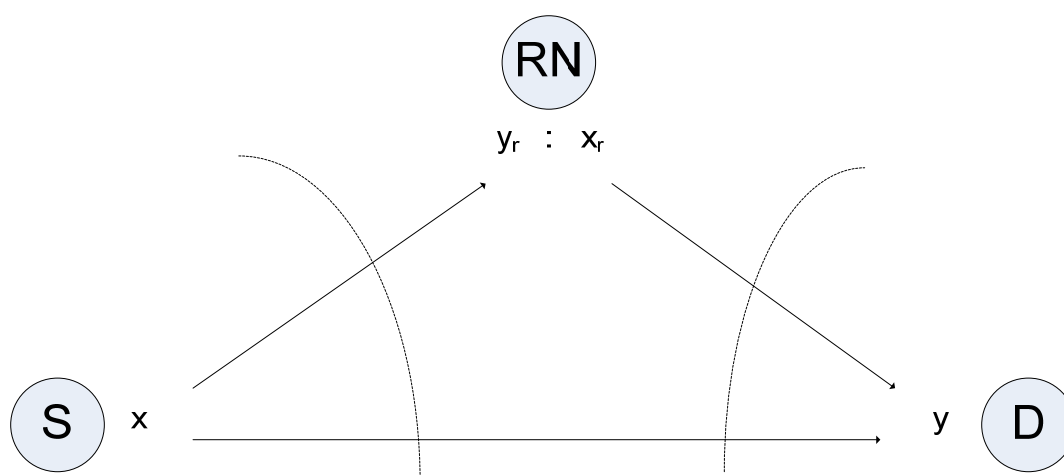


Figure 3.1. The relay channel

From the prospect of the information theory, the focus lies on the input-output relationship between the source and destination, expressed by random variables sets X and Y , respectively, and the relay enhances the wireless link by forward signal x_r to the destination, which is based on the its current or past receive signal y_r from the source.

[57] pointed out that the capacity of a relay channel is the supremum of the set of achievable rates as

$$C \leq \sup_{p(x, x_r)} \min \{I(X, X_r; Y), I(X; Y, Y_r | X_r)\}, \quad (3.1)$$

where $p(x, x_r)$ is the joint probability density function. The right side of the inequality (3.1) is called the cut-set upper bound for the relay channel. The term $I(X, X_r; Y)$ means the information rate from X and X_r to Y , which can be treated as the capacity of a multiple access channel from source and relay to destination. The term $I(X; Y, Y_r | X_r)$ means the information rate from X to Y and Y_r , which can be treated as the capacity of a broadcast channel from source to relay and destination.

3.2. Loop interference cancelling

In a Single Frequency Network (SFN) like LTE-Advanced, the communications among the eNBs, RNs and UEs are all supposed to be on the same frequency band, so that loop interference may occur at the RN when it is simultaneously receiving from the eNB and transmitting to the UE, or simultaneously receiving from the UE and transmitting to the eNB. Conventionally it is necessary to assign orthogonal resources, in time or in frequency, to separate the transmit and receive processes. In the early release of LTE, this work could be done with the MBSFN (Multi-Media Broadcast over a Single Frequency Network) subframe [116], which makes the RN work in half-duplex (HDX) mode by creating gaps for the eNB-RN transmissions. However, there are circuit technologies [10][75][95][101] to reduce the loop interference to a considerable low level by decoupling the RN's receive and transmit antennas, so that the RN is able to work on the full-duplex (FDX) mode, which contributes a lot in the capacity enhancement.

Figure 3.2 shows the basic concepts of cancelling the loop interference on the RN, which are illustrated in the frequency domain. The transmit signal interferes the receiving process on the RN's receive antenna as

$$R(\omega) = Y_r(\omega) + X_r(\omega)G(\omega)C(\omega), \quad (3.2)$$

where $Y_r(\omega)$ and $X_r(\omega)$ denote the receive and transmit signals' spectrums, $G(\omega)$ denotes the amplification function, $R(\omega)$ denotes the interfered signal and $C(\omega)$ denotes the transfer function of the coupling path from transmit antenna to receive antenna.

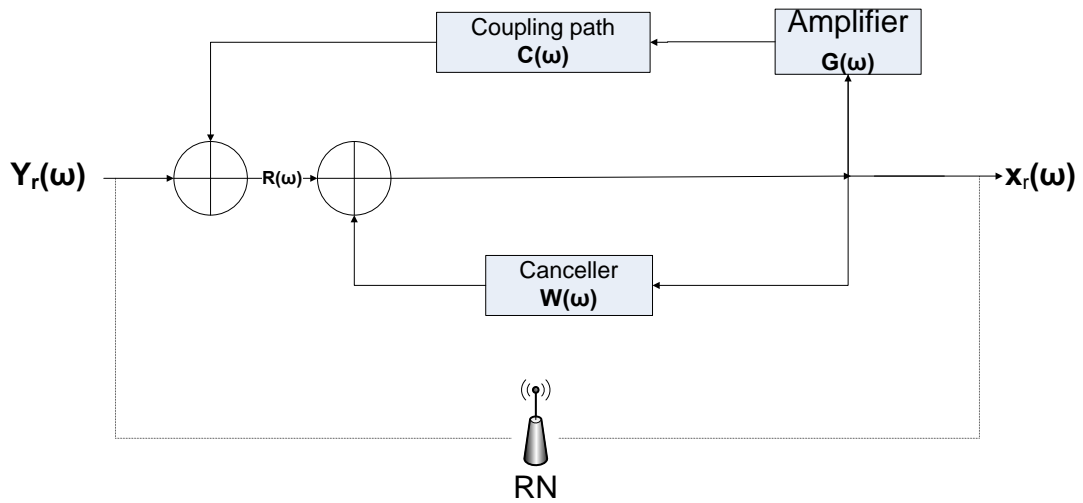


Figure 3.2. Loop Interference cancelling

[10] A canceller with the transfer function $W(\omega)$ is used for reducing this loop interference, then the equation should hold for the forward signal

$$X_r(\omega) = R(\omega) - X_r(\omega)W(\omega). \quad (3.3)$$

The system function is

$$H(\omega) = \frac{X_r(\omega)}{Y_r(\omega)} = \frac{1}{1 - (G(\omega)C(\omega) - W(\omega))}, \quad (3.4)$$

when $W(\omega) = G(\omega)C(\omega)$, the loop interference is fully cancelled.

3.3.Cooperative relaying

3.3.1.AF and DF

Coordinating the source and the relay in a wireless system, we can expect to achieve the multiplexing capacity of cooperative communications and obtain higher diversity gain by applying space-time coding [42][44][45][98][110].

The forward signal of the RN is the fixed-gain amplification of the current or past received signal (with or without noises), depending on the types of relaying and the length of processing time. Two basic types of relaying are investigated in this report, amplify-and-forward (AF) relaying and decode-and-forward (DF) relaying. AF and DF are two different forwarding strategies of the relay stations. AF relaying simply amplify the received analog signals and forward while some advanced AF relaying can also have control and measurement functions. AF relaying have already been used for handling the coverage holes in nowadays cellular networks. Compared to DF scheme, directly amplifying and forwarding introduces less delay in processing time but greater noises and interference in the system. On the other hand, for the DF relaying, decoding and re-encoding before forwarding the received data blocks can eliminate noises and interference but a significant delay should be noted.

Since the uplink and downlink transmissions of a relay network are quite symmetric, except the lower power of the UE's transmit antenna, here only the downlink phase is analyzed. In the downlink phase of a LTE-like network, the eNB acts as the source and the UE acts as the destination.

In the following, we refer to the connection between an eNB and an RN as relay link (RL), the connection between an RN and a UE as access link (AL), and the connection between an eNB and a UE as direct link (DL). h_{RL} , h_{AL} and h_{DL} are the channel gains for the RL link, the AL link and the DL link respectively. x and x_r are the signals transmitted by the eNB and the RN, respectively. Power levels on the eNB and RN are defined as $\mathcal{E}\{|x|^2\} = P_{eNB}$, $\mathcal{E}\{|x_r|^2\} = P_{RN}$, respectively, which forms a total power constraint that $P = P_{eNB} + P_{RN}$. n and n_r are the noises observed at the UE and the RN respectively, with variances σ^2 and σ_r^2 .

3.3.2.Half duplex relaying

Figure 3.3 illustrates the half duplex (HDX) mode, on which the RN could not receive any signal while it is transmitting and vice versa. As shown, it takes two steps (two time slots) to complete the transmission of one symbol [60].

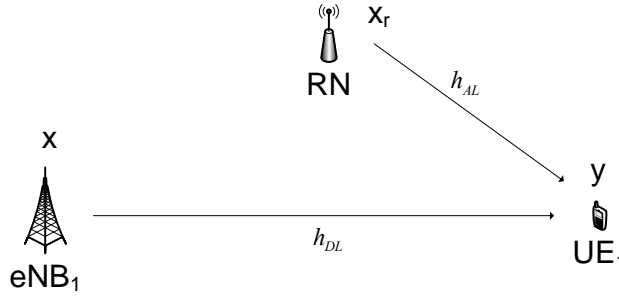
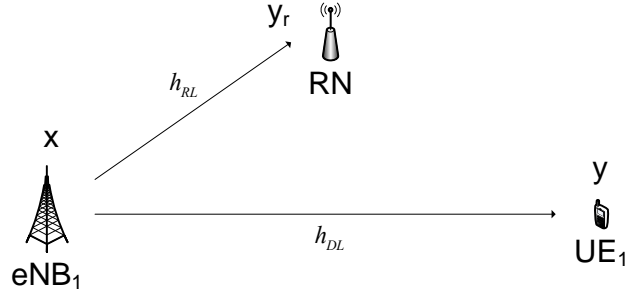


Figure 3.3. Half duplex relaying: transmissions in time slot $[i]$ (above) and time slot $[i + 1]$ (below)

In time slot $[i]$, the eNB broadcasts signal $x[i]$ to both the RN and the UE. The receive signal at RN is

$$y_r^{HDX}[i] = h_{RL}[i]x[i] + n_r[i], \quad (3.5)$$

and the receive signal at UE is

$$y^{HDX}[i] = h_{DL}[i]x[i] + n[i]. \quad (3.6)$$

In next time slot $[i + 1]$, the eNB sends signal $x[i + 1]$ and the RN stops receiving but transmitting $x_r^{HDX}[i + 1]$. The receive signal at UE is

$$y^{HDX}[i + 1] = h_{DL}[i + 1]x[i + 1] + h_{AL}[i + 1]x_r^{HDX}[i + 1] + n[i + 1], \quad (3.7)$$

where the transmit signal of the RN is a function of its past receive signals.

Assume the relay network described above are all located in a slow flat fading radio environment, then the channel gains and noises should be unchanged over both time slots $[i]$ and $[i + 1]$.

For a simple AF relay, the forward signal can be assumed as a fixed-gain amplification of the its receiving in the last time slot in the time domain, i.e.

$$x_r^{HDX}[i+1] = g_{AF} y_r^{HDX}[i], \quad (3.8)$$

where g_{AF} is the fixed gain scalar. Consider the power level of the RN,

$$g_{AF} = \sqrt{\frac{P_{RN}}{P_{eNB} |h_{RL}|^2 + \sigma_r^2}}, \quad (3.9)$$

where the denominator signifies the receive signal power at the RN.

Describe both time slots jointly and substitute (3.5) and (3.8) into (3.7), for HDX AF,

$$\underbrace{\begin{pmatrix} y_{AF}^{HDX}[i] \\ y_{AF}^{HDX}[i+1] \end{pmatrix}}_{\mathbf{y}} = \underbrace{\begin{pmatrix} h_{DL} & 0 \\ h_{AL} g_{AF} h_{RL} & h_{DL} \end{pmatrix}}_{\mathbf{H}} \underbrace{\begin{pmatrix} x[i] \\ x[i+1] \end{pmatrix}}_{\mathbf{x}} + \underbrace{\begin{pmatrix} n \\ h_{AL} g_{AF} n_r + n \end{pmatrix}}_{\mathbf{n}}. \quad (3.10)$$

Note that the elements in noise vector \mathbf{n} in (3.10) is not in the same scale. The noise power at the UE in time slot $[i+1]$ is

$$N_{UE}[i+1] = \sigma^2 \left(1 + |h_{AL}|^2 |g_{AF}|^2 \frac{\sigma_r^2}{\sigma^2} \right) = \sigma^2 \Lambda, \quad (3.11)$$

where N_{UE} denotes the noise power at UE and $\Lambda^{-1/2}$ denotes the scale factor.

Rewrite (3.10) by multiplying $\Lambda^{-1/2}$ on both sides

$$\underbrace{\begin{pmatrix} y_{AF}^{HDX}[i] \\ \Lambda^{-1/2} y_{AF}^{HDX}[i+1] \end{pmatrix}}_{\tilde{\mathbf{y}}} = \underbrace{\begin{pmatrix} h_{DL} & 0 \\ \Lambda^{-1/2} h_{AL} g_{AF} h_{RL} & \Lambda^{-1/2} h_{DL} \end{pmatrix}}_{\tilde{\mathbf{H}}} \underbrace{\begin{pmatrix} x[i] \\ x[i+1] \end{pmatrix}}_{\mathbf{x}} + \underbrace{\begin{pmatrix} n \\ \Lambda^{-1/2} (h_{AL} g_{AF} n_r + n) \end{pmatrix}}_{\tilde{\mathbf{n}}}, \quad (3.12)$$

where $\tilde{\mathbf{y}}$, $\tilde{\mathbf{H}}$ and $\tilde{\mathbf{n}}$ denote scaled version of receive signal vector, channel matrix and noise vector, respectively. The action of normalizing the noise power does not affect the evaluation of the mutual information but simplifies the ensuing presentation.

The mutual information of HDX AF relaying follows [60]

$$I_{AF}^{HDX} = \frac{1}{2} \log_2 \det \left(\mathbf{I} + \frac{P_{eNB}}{\sigma^2} \tilde{\mathbf{H}} \tilde{\mathbf{H}}^* \right), \quad (3.13)$$

where $\tilde{\mathbf{H}}$ is defined in (3.12) and the factor $\frac{1}{2}$ means averaging the capacity for one time slot.

For a simple DF relay, since the noise is cancelled during the decoding process, the forward signal can be then assumed as a fixed-gain amplification of the eNB's original transmit signal in the last time slot in the time domain, i.e.

$$x_r^{HDX}[i+1] = g_{DF} x[i], \quad (3.14)$$

where g_{DF} is the fixed gain scalar. Consider the power level of the RN,

$$g_{DF} = \sqrt{\frac{P_{RN}}{P_{eNB}}}, \quad (3.15)$$

where the denominator signifies the useful signal power without noises at the RN.

Describe both time slots jointly and substitute (3.5) and (3.14) into (3.7), for HDX DF,

$$\underbrace{\begin{pmatrix} y_{DF}^{HDX}[i] \\ y_{DF}^{HDX}[i+1] \end{pmatrix}}_{\mathbf{y}} = \underbrace{\begin{pmatrix} h_{DL} & 0 \\ h_{AL}g_{DF} & h_{DL} \end{pmatrix}}_{\mathbf{H}} \underbrace{\begin{pmatrix} x[i] \\ x[i+1] \end{pmatrix}}_{\mathbf{x}} + \underbrace{\begin{pmatrix} n \\ n \end{pmatrix}}_{\mathbf{n}}. \quad (3.16)$$

Different with HDX AF relaying, the upper bound of the information rate as shown in (3.13) may not be achievable for DF relaying due to the requirement of reliable decoding on the RN[60][127], which means the rate in time slot $[i]$ should not exceed the maximum information rate R_{RN} of the relay link (RL) for the RN to decode, i.e.

$$R_i \leq R_{RN} = \log_2 \left(1 + \frac{P_{eNB}}{\sigma^2} |h_{RL}|^2 \right), \quad (3.17)$$

where R_i denotes the rate for UE in the i th time slot.

Interestingly, the transmissions in two time slots as expressed in (3.16) form a MIMO MAC, which has been discussed in section 2.3.4. The capacity region of DF relaying is then

$$\begin{cases} R_i^{\max} = \log_2 \det \left(\mathbf{I} + \frac{P_{eNB}}{\sigma^2} \|\mathbf{h}_1\|^2 \right) \\ R_{i+1}^{\max} = \log_2 \det \left(\mathbf{I} + \frac{P_{eNB}}{\sigma^2} \|\mathbf{h}_2\|^2 \right) \\ R_{total} = \log_2 \det \left(\mathbf{I} + \frac{P_{eNB}}{\sigma^2} \mathbf{H}\mathbf{H}^* \right) \end{cases}, \quad (3.18)$$

where \mathbf{h}_1 and \mathbf{h}_2 are first and second column of matrix \mathbf{H} in equation (3.16). Any rate

pairs (R_i, R_{i+1}) satisfy the condition $\begin{cases} R_i \leq R_i^{\max} \\ R_{i+1} \leq R_{i+1}^{\max} \\ R_i + R_{i+1} \leq R_{total} \end{cases}$ are achievable in the network.

Note that the requirement of error-free decoding on the RN, the rate R_i should satisfy

$$R_i \leq \min(R_i^{\max}, R_{RN}). \quad (3.19)$$

The mutual information of HDX DF relaying is then

$$I_{DF}^{HDX} = \frac{1}{2} \min \{ R_{total}, R_{RN} + R_{i+1}^{max} \}, \quad (3.20)$$

where the factor $\frac{1}{2}$ shows the average capacity for one time slot.

3.3.3. Full duplex relaying

The full duplex (FDX) relaying mode, on which the RN can receive while it is transmitting and vice versa, is illustrated in figure 3.4. As shown, it takes at least one time slot (in the case of the AF RN on which the processing time can be ignored) to complete the transmission of one signal.

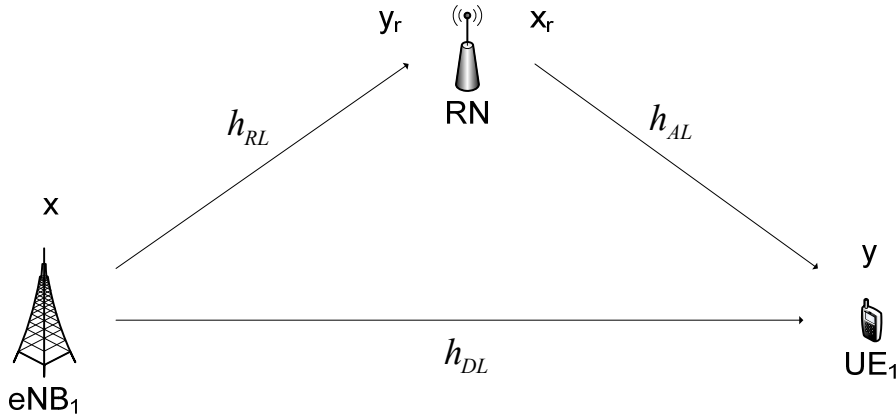


Figure 3.4. Full-duplex relaying

In time slot $[i]$, the eNB broadcasts to both the RN and the UE, meanwhile, the RN also transmits to the UE. The receive signal at RN is

$$y_r^{FDX}[i] = h_{RL}[i]x[i] + n_r[i], \quad (3.21)$$

and the receive signal at UE is

$$y^{FDX}[i] = h_{DL}[i]x[i] + h_{AL}[i]x_r^{FDX}[i] + n[i], \quad (3.22)$$

where the transmit signal of the RN is a function of its current/past receive signals.

For FDX AF relaying, the transmission of one signal $x[i]$ can be done in one time slot. Modifying (3.8) as $x_r^{HDX}[i] = g_{AF}y_r^{HDX}[i]$ and substitute it with (3.21) into (3.22), the receive signal at UE (assuming the channel is constant over two time slots) is

$$y_{AF}^{FDX}[i] = \underbrace{(h_{DL} + h_{AL}g_{AF}h_{RL})}_{\tilde{h}}x[i] + \underbrace{(h_{AL}g_{AF}n_r + n)}_{\tilde{n}}. \quad (3.23)$$

The mutual information of FDX AF relaying can be evaluated according to the Shannon theory for bandwidth-limited Gaussian channel, i.e.

$$I_{AF}^{FDX} = \log_2 \left(1 + \frac{P_{eNB} |\tilde{h}|^2}{\sigma^2 \Lambda} \right), \quad (3.24)$$

where \tilde{h} is defined in (3.23) and $\sigma^2 \Lambda$ is the noise power at the UE which is defined in (3.11).

For DF FDX, substitute (3.14) and (3.21) into (3.22), the receive signal in time slot $[i]$ at UE is

$$y_{DF}^{FDX}[i] = h_{DL}x[i] + h_{AL}g_{DF}x[i-1] + n. \quad (3.25)$$

In time slot $[i+1]$, similarly, the receive signal at UE is

$$y_{DF}^{FDX}[i+1] = h_{DL}x[i+1] + h_{AL}g_{DF}x[i] + n.$$

Describe both time slots jointly, for FDX DF relaying,

$$\underbrace{\begin{pmatrix} y_{DF}^{FDX}[i] \\ y_{DF}^{FDX}[i+1] \end{pmatrix}}_{\mathbf{y}} = \underbrace{\begin{pmatrix} h_{AL}g_{DF} & h_{DL} & 0 \\ 0 & h_{AL}g_{DF} & h_{DL} \end{pmatrix}}_{\mathbf{H}} \underbrace{\begin{pmatrix} x[i-1] \\ x[i] \\ x[i+1] \end{pmatrix}}_{\mathbf{x}} + \underbrace{\begin{pmatrix} n \\ n \end{pmatrix}}_{\mathbf{n}}. \quad (3.26)$$

Similar with the analysis for the HDX DF relaying in section 3.3.2, the requirement of reliable decoding on the RN should be satisfied in both time slots for FDX DF relaying, i.e.

$$I_{DF}^{FDX} = \frac{1}{2} \min \{ R_{total}, R_{RN} \}, \quad (3.27)$$

where $R_{total} = \log_2 \det \left(\mathbf{I} + \frac{P_{eNB}}{\sigma^2} \mathbf{H} \mathbf{H}^* \right)$ and $R_{RN} = \log_2 \left(1 + \frac{P_{eNB}}{\sigma^2} |h_{RL}|^2 \right)$, with \mathbf{H} defined in (3.26).

3.3.4. Numerical results

In this section, we run numerical simulations to compare the achievable capacities (for unit bandwidth) of relaying in four different configurations: HDX AF, HDX DF, FDX AF and FDX DF.

Firstly, we estimate the effects of relay link quality on the achievable rates in DF relaying

as mentioned in equation (3.17). We choose the receive SNR on the RL γ_{RL} as an independent variable, with 10dB receive SNR on DL $\gamma_{DL} = \frac{P_{eNB}}{\sigma^2} |h_{DL}|^2 = 10dB$ and 10dB receive SNR on AL $\gamma_{AL} = \frac{P_{RN}}{\sigma^2} |h_{AL}|^2 = 10dB$, where γ denotes the receive SNR. Assume that transmit powers $P_{eNB} = P_{RN}$, noise powers $\sigma^2 = \sigma_r^2$ and $\frac{P_{eNB}}{\sigma^2} = \frac{P_{RN}}{\sigma^2} = \frac{P_{eNB}}{\sigma_r^2} = 30dB$.

The channel gains h_{DL} and h_{AL} are the complex Gaussian distributed $\sim 0.1 \times \mathcal{CN}(0,1)$, indicating the Rayleigh fading environment and the factor 0.1 can be treated as attenuations caused by the path loss and shadowing. The receive SNR on RL is then $\gamma_{RL} = \frac{P_{eNB}}{\sigma_r^2} |h_{RL}|^2$, and the channel gain h_{RL} is the complex Gaussian distributed \sim

$\sqrt{10^{\frac{(\gamma_{RL}-3)}{10}}} \times \mathcal{CN}(0,1)$, where the factor $\sqrt{10^{\frac{(\gamma_{RL}-3)}{10}}}$ denotes the attenuation due to path loss and shadowing on the relay link.

According to equation (3.13)(3.20)(3.24)(3.27), for each channel realization h_{DL} , h_{RL} and h_{AL} we can the evaluations mutual information for HDX AF, HDX DF, FDX AF and FDX DF relaying. Repeat 1000 times and take the expectations, we can get the ergodic capacities for each of the relaying strategies.

Figure 3.5 shows the relationship of the capacity and the receive SNR of the relay link. When RL is not good enough ($\gamma_{RL} < 20$ dB approximately) the capacity of HDX AF relaying is higher than the capacity of HDX DF relaying and the capacity of FDX AF relaying is higher than the FDX DF relaying, which proves the fact that DF relaying is susceptible to the relay link quality. When RL is strong, DF relaying outperforms AF in capacities.

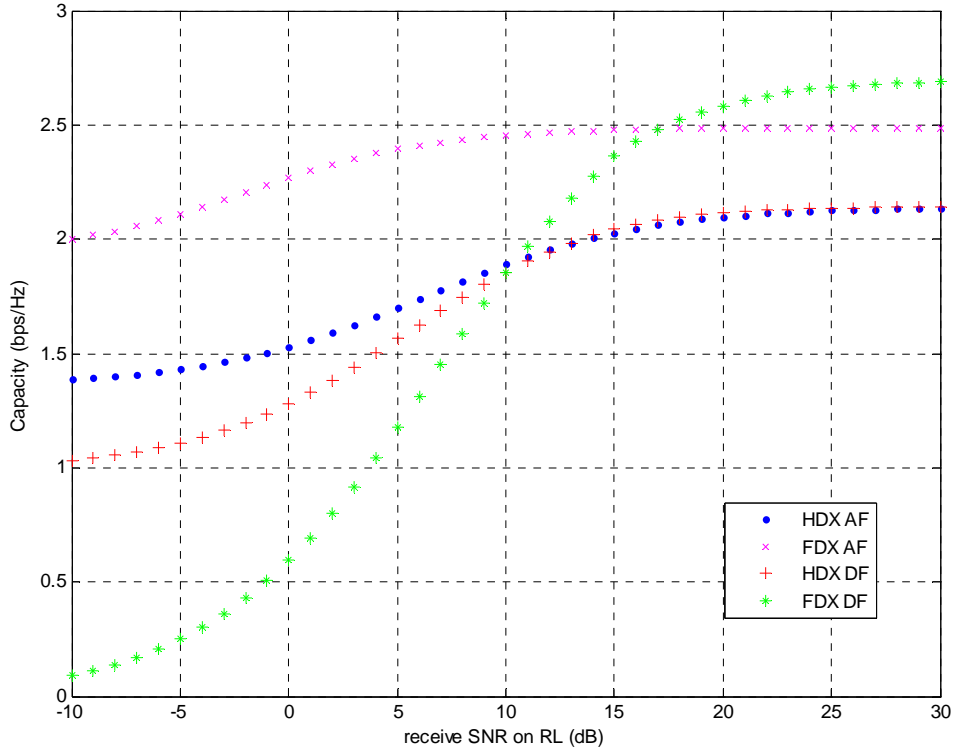


Figure 3.5. Capacity versus receive SNR of Relay Link: HDX AF, FDX AF, HDX DF and FDX DF

Next, we evaluate the effects access link quality on the achievable capacities. With average DL (10dB) and ideal RL (30dB), which means that channel gain h_{DL} is complex Gaussian distributed $\sim 0.1 \times \mathcal{CN}(0,1)$ and channel gains h_{RL} is complex Gaussian distributed $\sim \mathcal{CN}(0,1)$, figure 3.6 shows how the channel capacity changes with the receive SNR on the AL γ_{AL} , for which the channel gain h_{RL} is the complex Gaussian

distributed $\sim \sqrt{10^{\frac{(\gamma_{AL}-3)}{10}}} \times \mathcal{CN}(0,1)$. We can see from this figure that the capacity of FDX relaying is higher than the capacity of HDX relaying and DF relaying outperforms AF relaying because the noises are not amplified by the DF RN in the network.

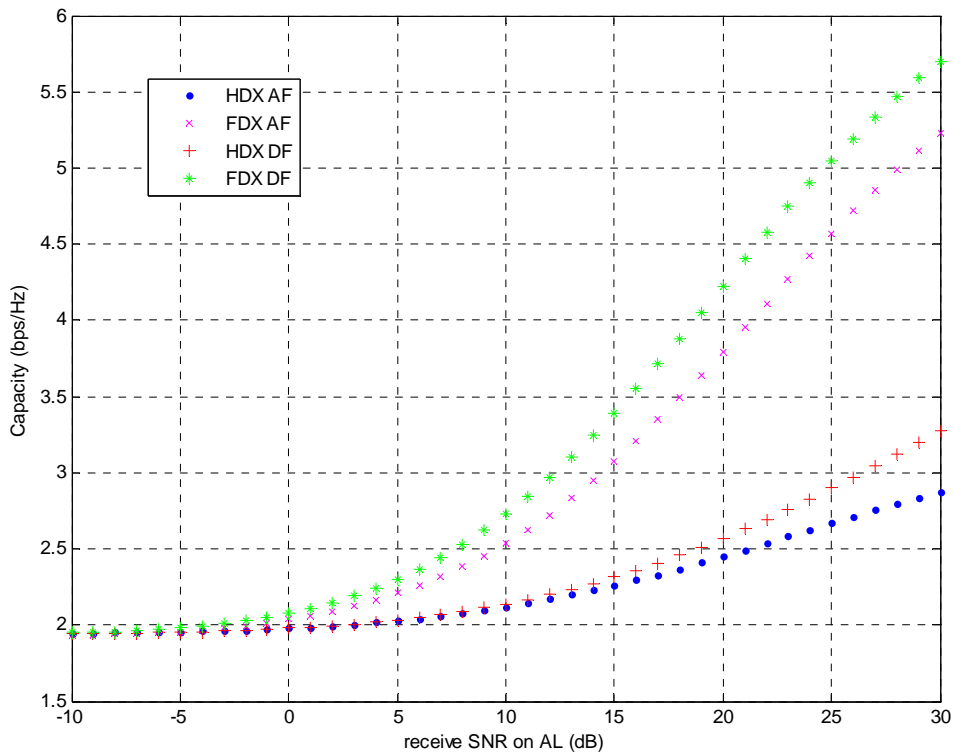


Figure 3.6. Capacity versus receive SNR of Access Link: HDX AF, FDX AF, HDX DF and FDX DF

3.4. Multi-antenna receiver

Other than equipping single antenna on all the devices in a relay network, it's interesting to investigate the multi-antenna devices. If the UE has two receive antennas, meanwhile, the eNB and the RN are cooperated perfectly (which means the RN should be a AF relay in full-duplex mode and the relay link can be considered as ideal), then the rank of the downlink channel matrix can be increased to two and the relay network can be modeled as a 2×2 MIMO with the geographically distributed inputs: one is from eNB, the other is from RN.

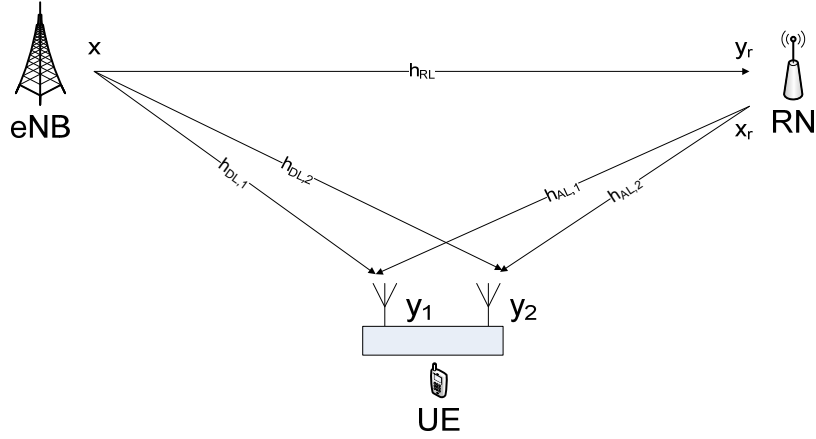


Figure 3.7. Downlink transmissions in a relay network with a 2-antenna UE

As illustrated in figure 3.7, considering eNB and RN forming a transmit array with two distributed antennas, we can describe the channel with a matrix $\begin{pmatrix} h_{DL,1} & h_{AL,1} \\ h_{DL,2} & h_{AL,2} \end{pmatrix}$. Since the

RN is FDX AF, according to (3.8)(3.9)(3.23) and analysis in section 3.3.3, the input-output relationship of this relay network is

$$\mathbf{y} = \underbrace{\begin{pmatrix} h_{DL,1} & h_{AL,1} \mathbf{g}_{AF} h_{RL} \\ h_{DL,2} & h_{AL,2} \mathbf{g}_{AF} h_{RL} \end{pmatrix}}_{\mathbf{H}} \underbrace{\begin{pmatrix} x \\ x \end{pmatrix}}_{\tilde{\mathbf{x}}} + \underbrace{\begin{pmatrix} h_{AL,1} \mathbf{g}_{AF} n_r + n \\ h_{AL,2} \mathbf{g}_{AF} n_r + n \end{pmatrix}}_{\tilde{\mathbf{n}}} \quad (3.28)$$

with receive signal vector at the UE $\mathbf{y} = \begin{pmatrix} y_1 \\ y_2 \end{pmatrix}$. Similar with (3.11), the elements in the noise vector \mathbf{n} in (3.28) should be scaled. Consider the noise power at the i th receive antenna of the UE,

$$N_i = \sigma^2 \left(1 + |h_{AL,i}|^2 |\mathbf{g}_{AF}|^2 \frac{\sigma_r^2}{\sigma^2} \right), \quad (3.29)$$

where $i = 1, 2$ for both of the UE's receive antennas.

Multiplying with the scale factor $N_i^{-1/2}$ on the corresponding receive signals and channel gains, (3.28) can be rewritten as

$$\underbrace{\begin{pmatrix} y_1 N_1^{-1/2} \\ y_2 N_2^{-1/2} \end{pmatrix}}_{\tilde{\mathbf{y}}} = \underbrace{\begin{pmatrix} h_{DL,1} N_1^{-1/2} & h_{AL,1} \mathbf{g}_{AF} h_{RL} N_1^{-1/2} \\ h_{DL,2} N_2^{-1/2} & h_{AL,2} \mathbf{g}_{AF} h_{RL} N_2^{-1/2} \end{pmatrix}}_{\mathbf{H}} \underbrace{\begin{pmatrix} x \\ x \end{pmatrix}}_{\tilde{\mathbf{x}}} + \underbrace{\begin{pmatrix} (h_{AL,1} \mathbf{g}_{AF} n_r + n) N_1^{-1/2} \\ (h_{AL,2} \mathbf{g}_{AF} n_r + n) N_2^{-1/2} \end{pmatrix}}_{\tilde{\mathbf{n}}}, \quad (3.30)$$

for which the capacity can be evaluated through the equation (2.8) introduced in section

2.3.2 for a MIMO system, i.e.

$$I_{2\text{-antenna UE}}^{FDXAF} = \log 2 \det(\mathbf{I} + P\mathbf{H}\mathbf{H}^*), \quad (3.31)$$

where the superscript $FDXAF$ denotes FDX AF relaying, \mathbf{H} is defined in (3.30) and $P = P_{\text{eNB}} = P_{\text{RN}}$ means that the RN is transmitting at the same power of the eNB's. Since the noise power is normalized, P here also denotes the SNR of each wireless link. With assumptions that $\sigma^2 = \sigma_r^2 = 1$ and all the channel gains are assumed to have the same quality and complex Gaussian distributed $\sim \mathcal{CN}(0,1)$, indicating a Rayleigh fading environment, we compare the capacities and outage performance of FDX AF relay networks with 2-antenna UE (3.31) and 1-antenna UE (3.24).

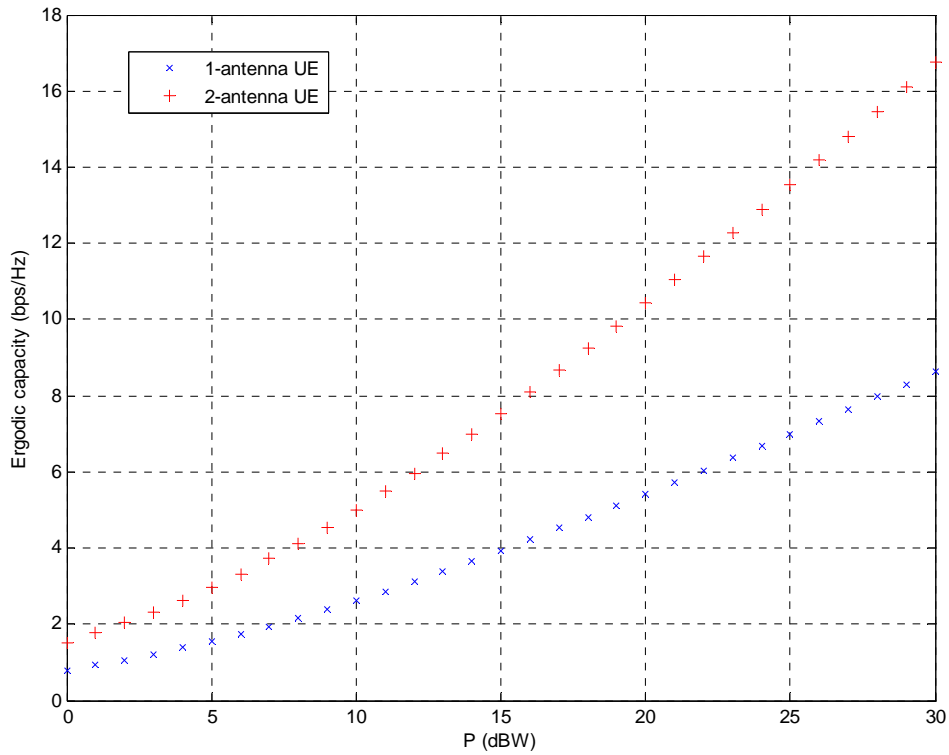


Figure 3.8. Capacities of 1- and 2-antenna UEs versus P

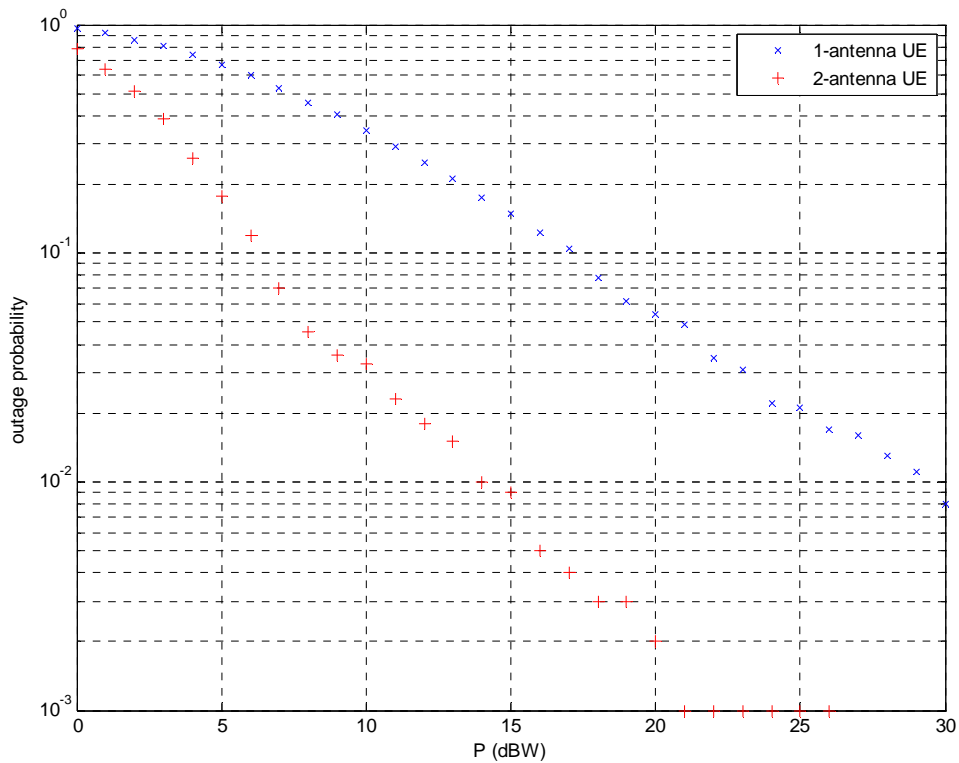


Figure 3.9. Outage probabilities (at $R=2\text{bps/Hz}$) of 1- and 2-antenna UEs versus P

Figure 3.8 compares the ergodic capacities of FDX AF relaying networks for single antenna UE and 2-antenna UE. From this figure, a significant improvement in capacity is shown when more antennas are used for transmitting and receiving. For a two-antenna UE, with every 3dB increase in SNR, it can gain 2 bps/Hz in capacity, which is almost the maximum multiplexing gain in a 2×2 MIMO system. And it is two times of the capacity gain in the system with single antenna UE.

Figure 3.9 compares the outage probabilities of FDX AF relaying networks for single antenna UE and 2-antenna UE. Lower outage probability can be obtained by adding one receive antenna on the UE. Moreover, with every 3dB increase in SNR, the outage probability decreases by a factor of 2^{-2} in the system with 2-antenna UE and a factor of 2^{-1} in the system with 1-antenna UE.

4

BASE STATION COORDINATION

For the cell-edge users, the inter-cell interference is the dominant factor of the performance degradations. To reduce or even utilize this interference, the tight co operations among the base stations are required. Traditionally, the scheduler would assign orthogonal resource to the adjacent cells to avoid the inter-cell interference. However, based on the multi-user information theory, particularly the multi-user MIMO technology, base station coordination can realize multi-user transmissions on each allocated resource block, which would significantly enlarge the system capacity.

Section 4.1 models the base station coordination in details. Section 4.2 emphases on the design of the pre-coding matrix. Section 4.3 evaluates the achievable sum-rate capacity in a two-cell system with base station coordination and compares the result with the capacity in the conventional system.

4.1. System model

Base station coordination enables adjacent cells to work on the same resource block. With multi-cell processing, the scheme can be consider as an extension of MIMO BC discussed in the section 2.3.4 with a distributed transmit antenna array in different cells and the inter-cell interference can be cancelled preliminarily on the transmitter side.

In the following, we refer to the connection between m th eNB and k th UE as direct link with channel gain $h_{DL,mk}$. The channels in the uplink are assumed to be the conjugate transposes of those in the downlink. $x_{eNB,m}$ and $x_{UE,k}$ are the signals transmitted by the m th eNB and the k th UE, respectively. $y_{eNB,m}$ and $y_{UE,k}$ are the receive signals at the m th eNB and the k th UE, respectively. $n_{eNB,m}$ and $n_{UE,k}$ are the noises observed at the m th eNB and the k th UE, respectively, with the same variance σ^2 .

Assuming that there are M eNBs and K UEs in the network and all the devices are equipped with single antenna, the channel is expressed in a $K \times M$ (or $M_R \times M_T$ if we count the numbers of receive and transmit antennas) matrix \mathbf{H} that

$$\mathbf{H} = \begin{pmatrix} h_{DL,11} & h_{DL,21} & \cdots & h_{DL,M1} \\ h_{DL,12} & h_{DL,22} & \cdots & h_{DL,M2} \\ \vdots & \vdots & \ddots & \vdots \\ h_{DL,1K} & h_{DL,2K} & \cdots & h_{DL,MK} \end{pmatrix}.$$

Similar with (2.20), the downlink transmissions can be modeled as

$$y_{UE,k} = \mathbf{h}_k \mathbf{x}_{eNB} + n_{UE,k}, \quad (4.1)$$

where \mathbf{h}_k is the channel from all the eNBs to the k th UE and equal to the k th row of \mathbf{H} , i.e.

$$\mathbf{h}_k = (h_{DL,1k} \quad h_{DL,2k} \quad \cdots \quad h_{DL,Mk}) \quad \text{and} \quad \mathbf{x}_{eNB} = \begin{pmatrix} x_{eNB,1} \\ x_{eNB,2} \\ \vdots \\ x_{eNB,M} \end{pmatrix} \quad \text{is the transmit signal vector from}$$

the eNBs and the total power of the transmit antennas is limited as P_{eNB} , i.e.

$$\mathcal{E}\{\mathbf{x}_{eNB}^* \mathbf{x}_{eNB}\} \leq P_{eNB}.$$

And the uplink transmissions can be modeled as in (2.19)

$$\mathbf{y}_{eNB} = \mathbf{H}^* \mathbf{x}_{UE} + \mathbf{n}_{eNB}, \quad (4.2)$$

where \mathbf{H}^* is the MAC channel from all the UEs to the eNBs, $\mathbf{x}_{UE} = \begin{pmatrix} x_{UE,1} \\ x_{UE,2} \\ \vdots \\ x_{UE,K} \end{pmatrix}$ is the

transmit signal vector from the UEs and the total power of the transmit antennas is

limited as P_{UE} , i.e. $\mathcal{E}\{\mathbf{x}_{UE}^* \mathbf{x}_{UE}\} \leq P_{UE}$. $\mathbf{n}_{eNB} = \begin{pmatrix} n_{eNB,1} \\ n_{eNB,2} \\ \vdots \\ n_{eNB,M} \end{pmatrix}$ is the noise vector which consists

of noises at each eNB's receive antenna.

4.2.Pre-coding in the downlink phase

Considering the downlink transmissions, since the eNBs are coordinated in the network, which indicates that the signal transmitted by each eNB may contain information

intended to multiple UEs, the transmit signal vector \mathbf{x}_{eNB} could be constructed as [49][51][126]

$$\mathbf{x}_{eNB} = \mathbf{W}\mathbf{d}, \quad (4.3)$$

where $\mathbf{d} = \begin{pmatrix} d_1 \\ d_2 \\ \vdots \\ d_K \end{pmatrix}$ is the data symbol vector, in which d_k is specific data symbol intended

for the k th UE, with unit power, i.e., $\varepsilon\{\mathbf{d}\mathbf{d}^*\} = \mathbf{I}$, and

$$\mathbf{W} = \begin{pmatrix} \omega_{11} & \omega_{21} & \cdots & \omega_{K1} \\ \omega_{12} & \omega_{22} & \cdots & \omega_{K2} \\ \vdots & \vdots & \ddots & \vdots \\ \omega_{1M} & \omega_{2M} & \cdots & \omega_{KM} \end{pmatrix} \quad (4.4)$$

is the $M \times K$ pre-coding weights matrix. These weights assign the data symbols with different amplitudes and phases (or transmit powers). For the k th UE, all the other data symbols d_i ($i \neq k$) are considered as interference. When all the interference is eliminated, the k th UE only receives data symbol d_k , then multi-user transmissions are achieved. This is one of most important features of the base station coordination technology.

The pre-coding process is shown in figure 4.1. Although the base station coordination deconstructs the channel into parallel and independent channels by the pre-coding procedure, the individual UE could not cooperatively receive and decode. That means, the post processing as indicated in section 2.3.2 for single-user MIMO does not exist anymore and the actual entity which plays the role of the decoder is the wireless channel.

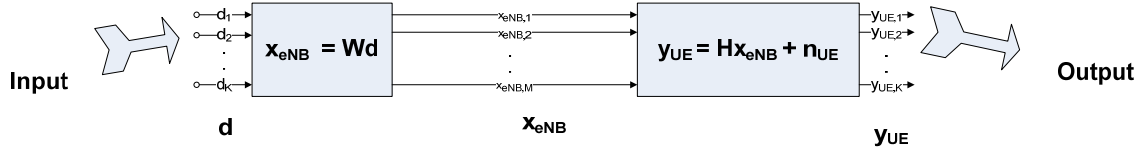


Figure 4.1. The pre-coding process in base station coordination

An important issue of base station coordination is the design of the pre-coding weight matrix \mathbf{W} . Other than the dirty paper coding technology introduced in [48][119], which can approach the theoretical bound of broadcast channel with high complexity, in this report, zero-forcing pre-coding [126] is discussed. Starting from an overview of the

downlink transmissions, rewrite (4.1) as

$$\mathbf{y}_{UE} = \mathbf{H}\mathbf{W}\mathbf{d} + \mathbf{n}_{UE}, \quad (4.5)$$

where $\mathbf{y}_{UE} = \begin{pmatrix} y_{UE,1} \\ y_{UE,2} \\ \vdots \\ y_{UE,K} \end{pmatrix}$ is the receive signal vector at UEs and $\mathbf{n}_{UE} = \begin{pmatrix} n_{UE,1} \\ n_{UE,2} \\ \vdots \\ n_{UE,K} \end{pmatrix}$ is the noise

vector observed by all the UEs.

If we want to establish a system that each UE only receives the data intended to it without any other multi-user interference, the products of matrixes $\mathbf{H} \times \mathbf{W}$ should be diagonal, i.e.

$$\mathbf{A} = \mathbf{H}\mathbf{W}, \quad (4.6)$$

where $\mathbf{A} = \text{diag}(a_1, \dots, a_K)$ is a $K \times K$ diagonal matrix.

With perfect channel knowledge at the transmitters, a straightforward approach is taking the channel inversion of matrix \mathbf{H}^{-1} to be a candidate of the pre-coding matrix \mathbf{W} , when $M = K$ (or $M_R = M_T$), i.e., the number of transmitters equals the number of receivers in the system,

$$\mathbf{W} = a\mathbf{H}^{-1}, \quad (4.7)$$

where a scalar a is for adjusting the antenna power to satisfy the total power constraint on the transmit antennas $\mathcal{E}\{\mathbf{x}_{eNB}^* \mathbf{x}_{eNB}\} \leq P_{eNB}$.

When $K < M$ (or $M_R < M_T$), we can take the similar action but replacing the inverse by pseudo-inverse, i.e.

$$\mathbf{W} = a\mathbf{H}^+. \quad (4.8)$$

Assume that \mathbf{H} is full rank, one simple method of obtaining the pseudo-inverse is taking

$$\mathbf{H}^+ = \mathbf{H}^* (\mathbf{H}\mathbf{H}^*)^{-1}, \quad (4.9)$$

since $\mathbf{H}\mathbf{H}^*$ generates a square matrix which always has an inverse.

However, if $K > M$ (or $M_R > M_T$), we could not get the accurate pseudo-inverse matrix through the method in (4.9). One simple and feasible solution is that we divide all the users into small groups in which the number of receivers is less than the number of transmitters. In LTE-like cellular network, different user groups can operate on different resource blocks and it's the task of scheduler to determine the subgroups and resource assignments.

In a more general sense, from the individual user point of view, we can rewrite (4.1) as

$$y_{UE,k} = \mathbf{h}_k \sum_{k=1}^K \mathbf{w}_k d_k + n_{UE,k}, \quad (4.10)$$

where $M \times 1$ vector \mathbf{w}_k stands for k th column of the pre-coding matrix \mathbf{W} .

Note that for the k th UE, any signals contain the symbols d_i ($i \neq k$) will be treated as interference, then the SINR for the k th UE is

$$SINR_k = \frac{|\mathbf{h}_k \mathbf{w}_k|^2 |d_k|^2}{\sigma_{n_{UE,k}}^2 + \sum_{i \neq k} |\mathbf{h}_k \mathbf{w}_i|^2 |d_i|^2}, \quad (4.11)$$

where $\sigma_{n_{UE,k}}^2$ denotes the noise power observed at the k th UE and the sum-rate capacity is the sum of achievable rates of all UEs, which can be estimated by equation (2.5).

For the purpose of eliminating all the multi-user interference, the zero-forcing conditions should be satisfied as

$$\mathbf{h}_k \mathbf{w}_i = 0, \text{ for any } i \neq k. \quad (4.12)$$

[126] Define $(K - 1) \times M$ (or $(M_R - 1) \times M_T$) matrix

$$\tilde{\mathbf{H}}_k = (\mathbf{h}_1 \quad \cdots \quad \mathbf{h}_{k-1} \quad \mathbf{h}_{k+1} \quad \cdots \quad \mathbf{h}_K)^T, \quad (4.13)$$

then we can transform the zero-forcing constraints to the condition that \mathbf{w}_k lies in the null space of $\tilde{\mathbf{H}}_k$. By this definition the k th UE receives its own data if the dimension of the $\tilde{\mathbf{H}}_k$ null space is larger than 0, i.e.

$$\dim(\ker(\tilde{\mathbf{H}}_k)) > 0. \quad (4.14)$$

There are several ways of finding \mathbf{w}_k by deciding null space of $\tilde{\mathbf{H}}_k$ such as singular value decomposition (SVD) or QR decomposition with column pivoting. [13][14]

In the uplink phase, all the UEs are assumed to be independent, so that pre-coding is not possible for the transmitters. However, the eNBs are coordinated and multi-user detection (MUD) [57] can be done on the receiver side.

4.3.Capacity improvement in the two-cell case

In this section we first establish a conventional network as a reference system for the further comparisons. We limit the analysis in a simple two-cell network to highlight the performance improvement of base station coordination and the results is ready to extended to the cases with more cells.

4.3.1.Conventional network

In a conventional cellular network, each eNB serves UEs in its own cell, with neither relays nor any kinds of coordinations. In a interference-free network, the resources allocated for different cells should be orthogonal. Assuming that transmissions in adjacent cells are time divided, without loss of generality, transmissions are following numerical orders. For example, in figure 4.2, black line denotes the transmission in the first time slot (for cell 1) and red line denotes the transmission in the second time slot (for cell 2).

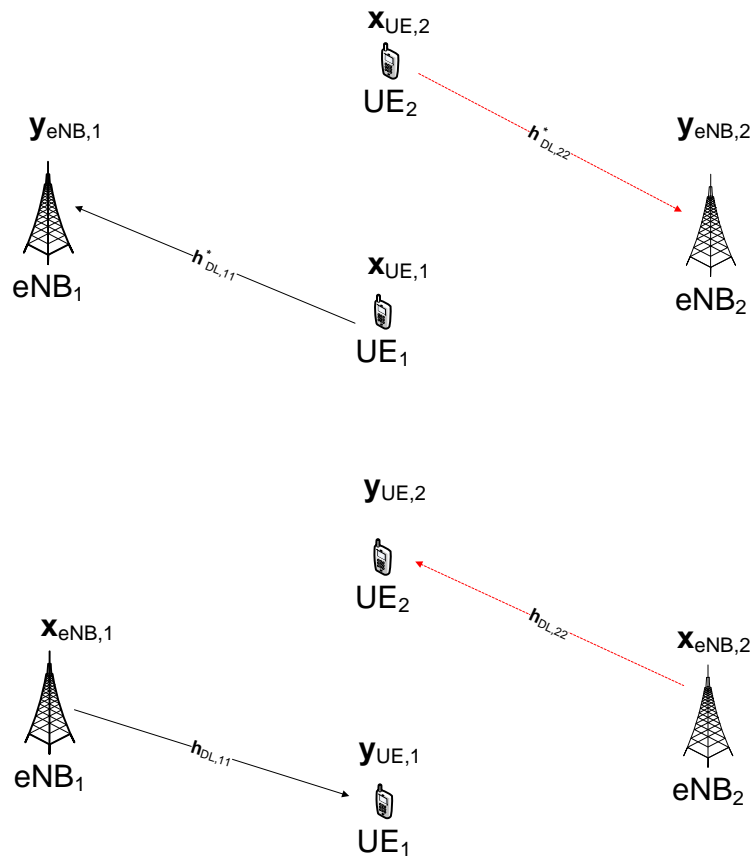


Figure 4.2.Uplink (above) and downlink (below) transmissions in a conventional network

For the uplink transmissions, in the first time slot $[i]$, the received signal at eNB₁ is

$$y_{eNB,1}[i] = h_{DL,11}^*[i]x_{UE,1}[i] + n_{eNB,1}[i]. \quad (4.15)$$

In the next time slot $[i + 1]$, the received signal at eNB₂ is

$$y_{eNB,2}[i + 1] = h_{DL,22}^*[i + 1]x_{UE,2}[i + 1] + n_{eNB,2}[i + 1]. \quad (4.16)$$

Assuming the channel gains stay unchanged over two time slots $[i]$ and $[i + 1]$, for a unit bandwidth, the sum-rate capacity of this conventional network is the average of rates in two time slots, which can be estimated according to equation (2.4),

$$C_{CON}^{UL} = \frac{1}{2} \left(\log_2 \left(1 + \frac{P_{UE}}{\sigma^2} |h_{DL,11}^*|^2 \right) + \log_2 \left(1 + \frac{P_{UE}}{\sigma^2} |h_{DL,22}^*|^2 \right) \right), \quad (4.17)$$

where a factor $\frac{1}{2}$ is for averaging over the two time slots, subscript *CON* denotes the conventional network, P_{UE} is total transmit power that UE could be assigned. σ^2 denotes the noise power.

The expression of sum-rate capacity is dual in the downlink transmissions, expect replacing the P_{UE} with P_{eNB} , which is the total power could be allocated by the eNB, i.e.

$$C_{CON}^{DL} = \frac{1}{2} \left(\log_2 \left(1 + \frac{P_{eNB}}{\sigma^2} |h_{DL,11}|^2 \right) + \log_2 \left(1 + \frac{P_{eNB}}{\sigma^2} |h_{DL,22}|^2 \right) \right). \quad (4.18)$$

4.3.2. Base station coordination in the two-cell case

According to the system model described in section 4.1, a two-cell network applying base station coordination technology is illustrated in figure 4.3. Note that in both uplink and downlink phases, two cells can operate simultaneously on the same frequency because the inter-cell interference is cancelled by the ZF pre-coding procedure on the eNBs.

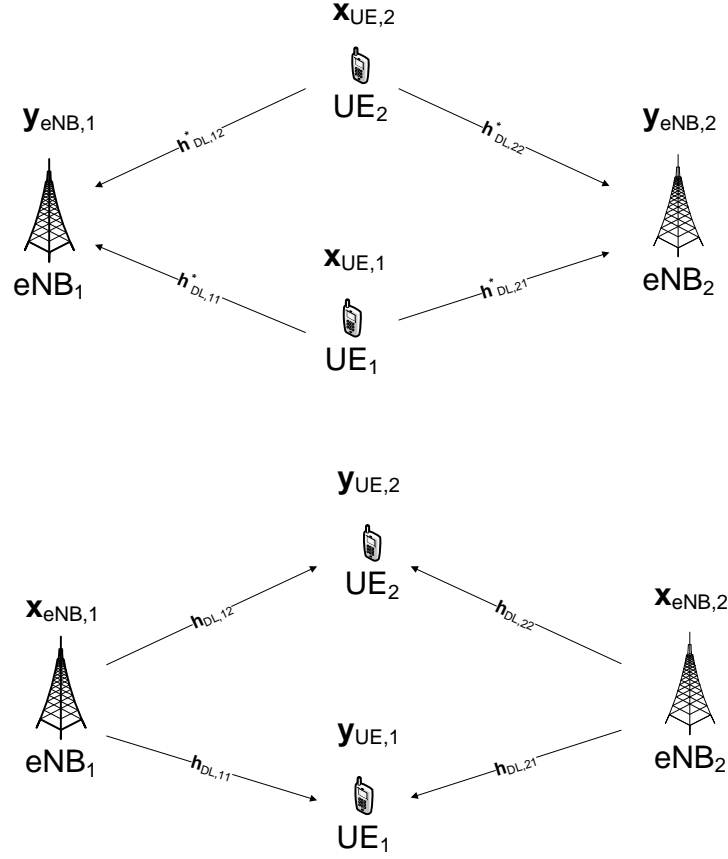


Figure 4.3. Uplink (above) and downlink (below) transmissions with base station coordination

Assuming that there are 2 eNBs and 2 UEs in the network and all the devices are equipped with single antenna, the channel is expressed in a 2×2 matrix \mathbf{H} that

$$\mathbf{H} = \begin{pmatrix} h_{DL,11} & h_{DL,21} \\ h_{DL,12} & h_{DL,22} \end{pmatrix}. \quad (4.19)$$

According to the (4.1)(4.3)(4.4), the downlink transmissions in this network can be expressed as

$$\begin{cases} y_{UE,1} = (h_{DL,11}\omega_{11} + h_{DL,21}\omega_{12})d_1 + (h_{DL,11}\omega_{21} + h_{DL,21}\omega_{22})d_2 + n_{UE,1} \\ y_{UE,2} = (h_{DL,12}\omega_{11} + h_{DL,22}\omega_{12})d_1 + (h_{DL,12}\omega_{21} + h_{DL,22}\omega_{22})d_2 + n_{UE,2} \end{cases}, \quad (4.20)$$

where the useful signals for UE₁ are expressed by $(h_{DL,11}\omega_{11} + h_{DL,21}\omega_{12})d_1$ and interference is $(h_{DL,11}\omega_{21} + h_{DL,21}\omega_{22})d_2$. For UE₂, the useful signals are $(h_{DL,12}\omega_{11} + h_{DL,22}\omega_{12})d_1$ and inferences are $(h_{DL,12}\omega_{21} + h_{DL,22}\omega_{22})d_2$.

As mentioned in section 4.1, the maximum allowed power of the eNBs is P_{eNB} , and here we restrict power allocations for each eNB as

$$\begin{cases} \mathcal{E}\left\{\left(\omega_{11}d_1 + \omega_{21}d_2\right)^2\right\} \leq P_{\text{eNB},1} \\ \mathcal{E}\left\{\left(\omega_{12}d_1 + \omega_{22}d_2\right)^2\right\} \leq P_{\text{eNB},2} \end{cases}, \quad (4.21)$$

where $P_{\text{eNB}} = P_{\text{eNB},1} + P_{\text{eNB},2}$.

According to the zero-forcing pre-coding algorithm, only under the circumstance that all the interference is removed the multi-user transmissions can be reliable, which means the following equalities must be satisfied

$$\begin{cases} h_{DL,11}\omega_{21} + h_{DL,21}\omega_{22} = 0 \\ h_{DL,12}\omega_{11} + h_{DL,22}\omega_{12} = 0 \end{cases}. \quad (4.22)$$

(4.21) and (4.22) is sufficient to define the weights in the pre-coding matrix \mathbf{W} and it is possible to find an optimization value of this matrix to maximize the sum rates.

According to the relationship between the information rate and SNR as indicated in (2.4), for individual UE, the rate should satisfy

$$\begin{cases} R_1 \leq \log_2 \left(1 + \frac{|h_{DL,11}\omega_{11} + h_{DL,21}\omega_{12}|^2}{\sigma^2} \right) \\ R_2 \leq \log_2 \left(1 + \frac{|h_{DL,12}\omega_{21} + h_{DL,22}\omega_{22}|^2}{\sigma^2} \right) \end{cases}, \quad (4.23)$$

where R_1 and R_2 denote the rates for UE₁ and UE₂ respectively. And the sum-rate capacity is then

$$C_{\text{BSC}}^{\text{DL}} = \log_2 \left(1 + \frac{|h_{DL,11}\omega_{11} + h_{DL,21}\omega_{12}|^2}{\sigma^2} \right) + \log_2 \left(1 + \frac{|h_{DL,12}\omega_{21} + h_{DL,22}\omega_{22}|^2}{\sigma^2} \right), \quad (4.24)$$

where the subscript BSC denotes the base station coordination.

In the uplink phase, as shown in figure 4.3, the uplink transmission can be modeled as in (4.2)

$$\underbrace{\begin{pmatrix} y_{\text{eNB},1} \\ y_{\text{eNB},2} \end{pmatrix}}_{\mathbf{y}_{\text{eNB}}} = \underbrace{\begin{pmatrix} h_{DL,11}^* & h_{DL,12}^* \\ h_{DL,21}^* & h_{DL,22}^* \end{pmatrix}}_{\mathbf{H}^*} \underbrace{\begin{pmatrix} x_{\text{UE},1} \\ x_{\text{UE},2} \end{pmatrix}}_{\mathbf{x}_{\text{UE}}} + \underbrace{\begin{pmatrix} n_{\text{eNB},1} \\ n_{\text{eNB},2} \end{pmatrix}}_{\mathbf{n}_{\text{eNB}}}, \quad (4.25)$$

where $\mathbf{H}^* = (\mathbf{h}_1^* \quad \mathbf{h}_2^*)$ is the conjugate transpose of the downlink MIMO BC channel \mathbf{H} in (4.19). Here we restrict the individual power $\varepsilon \left\{ (x_{UE,i})^2 \right\} = P_{UE,i}$ for i th UE, and $P_{UE} = P_{UE,1} + P_{UE,2}$, where P_{UE} is the maximum allowed power of UEs. As indicated in (2.21), the capacity region of the MIMO MAC uplink transmission is the union of

$$C_{MAC}(P_{UE}; \mathbf{H}^*) = \bigcup \left\{ \begin{array}{l} R_1 \leq \log_2 \det \left(\mathbf{I} + \mathbf{h}_1^* \frac{P_{UE,1}}{\sigma^2} \mathbf{h}_1 \right) \\ R_2 \leq \log_2 \det \left(\mathbf{I} + \mathbf{h}_2^* \frac{P_{UE,2}}{\sigma^2} \mathbf{h}_2 \right) \\ R_1 + R_2 \leq \log_2 \det \left(\mathbf{I} + \mathbf{h}_1^* \frac{P_{UE,1}}{\sigma^2} \mathbf{h}_1 + \mathbf{h}_2^* \frac{P_{UE,2}}{\sigma^2} \mathbf{h}_2 \right) \end{array} \right\}, \quad (4.26)$$

where the R_1, R_2 are the rates for two UEs separately and \mathbf{h}_1^* and \mathbf{h}_2^* are the first and second column of \mathbf{H}^* defined in (4.25).

According to equation (4.26), the sum-rate capacity in the uplink phase can be expressed as

$$C_{BSC}^{UL} = \log_2 \det \left(\mathbf{I}_2 + \mathbf{h}_1^* \frac{P_{UE,1}}{\sigma^2} \mathbf{h}_1 + \mathbf{h}_2^* \frac{P_{UE,2}}{\sigma^2} \mathbf{h}_2 \right). \quad (4.27)$$

4.3.3. Numerical results

In this section, we run numerical simulations to compare the achievable capacities (for unit bandwidth) of base station coordination in section 4.3.2 with the conventional system in section 4.3.1. The channel gains are all assumed i.i.d. complex Gaussian $\sim \mathcal{CN}(0,1)$, which indicates the ideal Rayleigh fading environment. The noises in the network are assumed to be additive and with variances $\sigma^2 = 0$ dBW. For statistic channel coefficients, the expected capacity is the average of sum-rate capacities in each channel realization (1000 times), which can be calculated by equation (4.17), (4.18), (4.24) and (4.27) accordingly. For simplicity, the power levels are assumed to be equal for all the eNBs or UEs, i.e. $P_{eNB,1} = P_{eNB,2} = \frac{1}{2} P_{eNB}$ and $P_{UE,1} = P_{UE,2} = \frac{1}{2} P_{UE}$. The independent variable chosen here is P_{eNB} (or P_{UE} in the uplink phase), since the noises are assumed to be unit, P_{eNB} (P_{UE}) is also an index of SNR on each parallel channel.

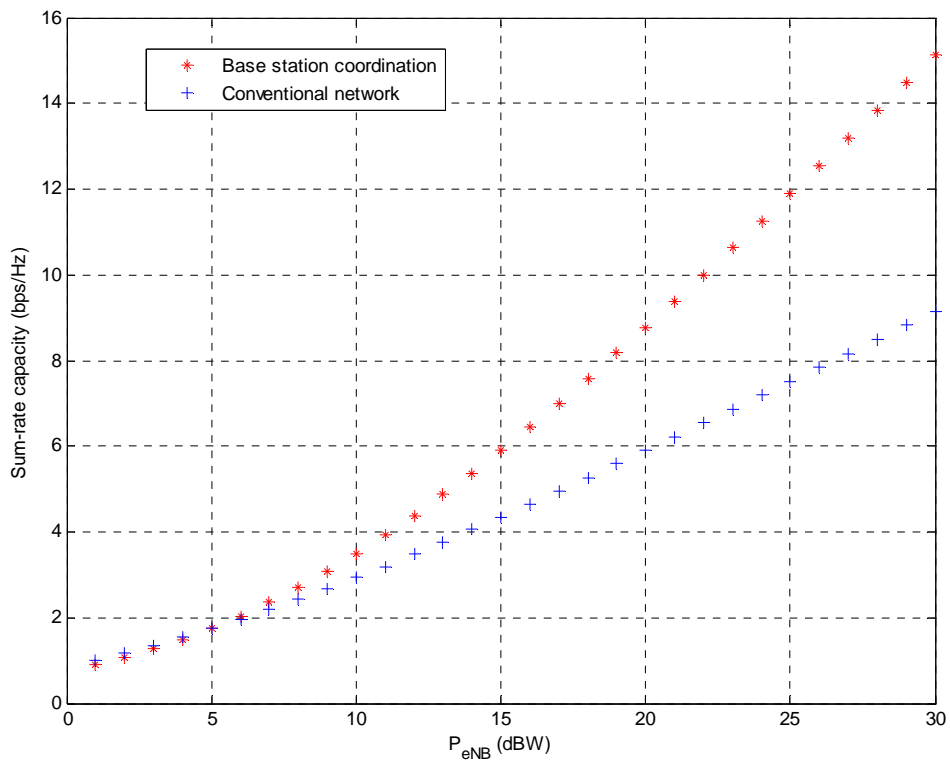
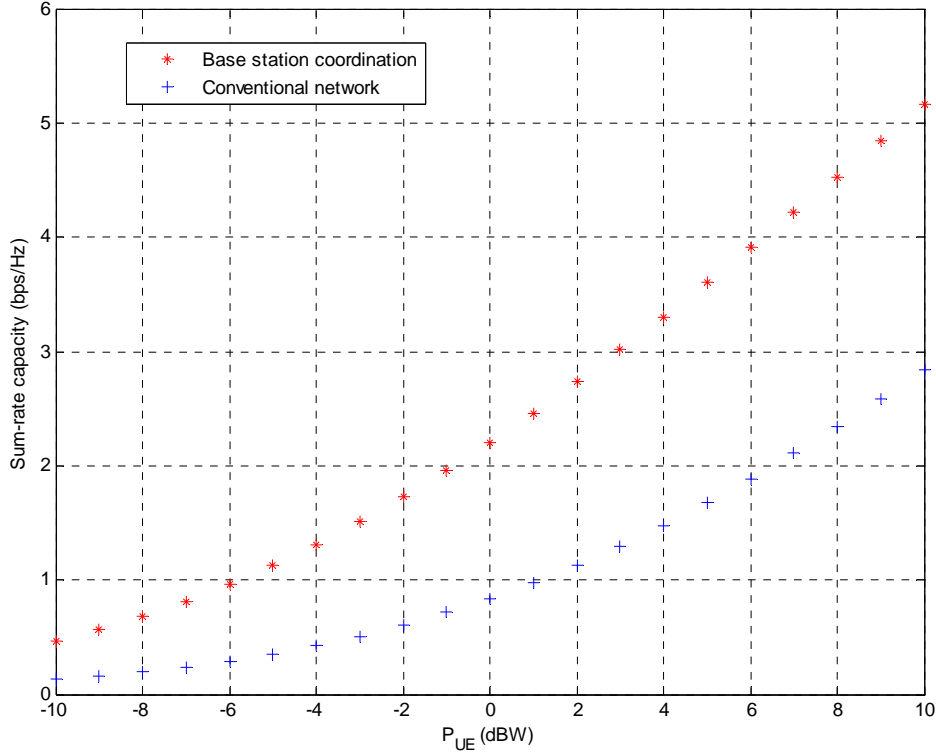


Figure 4.4. Downlink sum-rate capacity versus P_{eNB} : conventional and base station coordination


 Figure 4.5. Uplink sum-rate capacity versus P_{UE} : conventional and base station coordination

From figure 4.4 and 4.5 the advantage of base station coordination over the conventional time divided transmission scheme is shown visibly. In the downlink phase, in the case of high SNR, for every 3dB increase in SNR, the base station coordination with zero-forcing pre-coding can reach two times of the sum-rate capacity gain (2 bps/Hz) comparing with the conventional system (1 bps/Hz); in the case of low SNR, the capacity of base station coordination is nearly the same or even lower than the capacity of the conventional system, which indicates that zero-forcing pre-coding is sub-optimal. The reason is that in base station coordination, the allocated power is not fully used to transmit the useful signal. For example, with $P_{eNB} = 0$ dBW = 1 W, so that the individual power is $P_{eNB,1} = P_{eNB,2} = \frac{1}{2} P_{eNB} = 0.5$ W. For a random realization, the channel matrix is

$$\mathbf{H} = \begin{pmatrix} 0.1044 + 0.0093i & -0.5572 - 0.4195i \\ 0.2087 + 0.9722i & 0.1993 + 0.3443i \end{pmatrix}, \text{ and the corresponding pre-coding matrix}$$

$$\text{is } \mathbf{W} = \begin{pmatrix} 0.1717 - 0.2229i & 0.1247 - 0.4772i \\ -0.5799 + 0.3977i & -0.0220 - 0.0708i \end{pmatrix}. \text{ We can calculate that the actual transmit}$$

power of 1th eNB is 0.3224 W, and the actual transmit power of 2th eNB is 0.5 W. There

is a power penalty of 0.1776 W of base station coordination for this channel realization, which results in a degradation of the sum-rate capacity. In the uplink phase, the base station coordination reaches higher capacity for both low and high SNR in the network, the reason of which is the receivers (eNBs) can cooperatively decode so that all the receive signals are considered as useful ones. The system gains from the multiplexing, and the complexity lies on the pre- or post- processes which require channel status information on the eNBs.

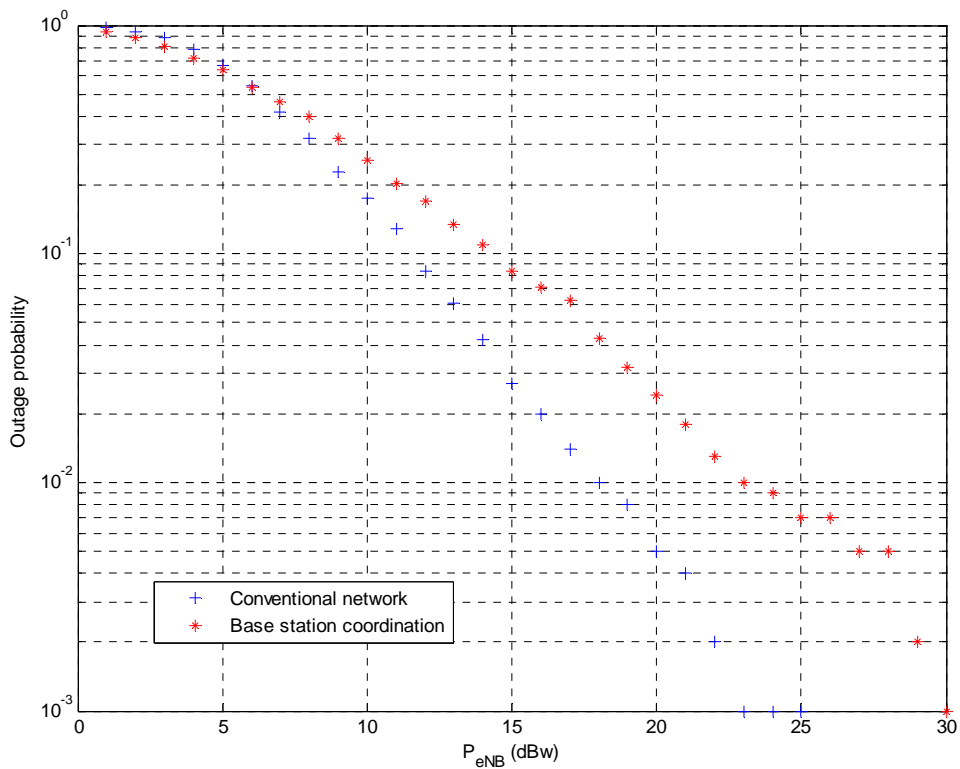


Figure 4.6. Downlink outage probability (at $R=2\text{bps/Hz}$) versus P_{eNB} : conventional and base station coordination

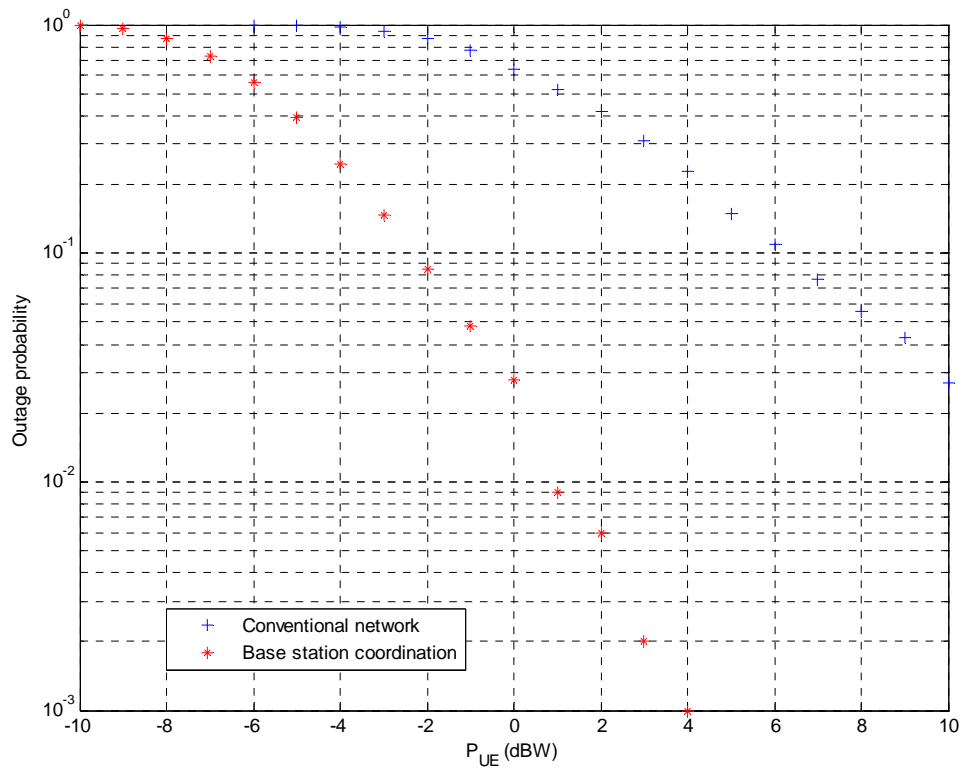


Figure 4.7. Uplink outage probability (at $R=1\text{bps/Hz}$) versus P_{UE} : conventional and base station coordination

Figure 4.6 and figure 4.7 show the outage probabilities in the downlink and uplink phase respectively. In the uplink phase, it is clear that the coordinated eNBs can reach the lower outage probability than the conventional system. However, in the downlink phase, the zero-forcing method does not have gains for base station coordination technology.

Because of the uplink-downlink duality introduced in section 2.3.4 and the equation (2.21), we can interpret the theoretical sum-rate capacity for the downlink transmission, which is in the same form as equation (4.27) by replacing power of UEs P_{UE} and power of eNBs P_{eNB} .

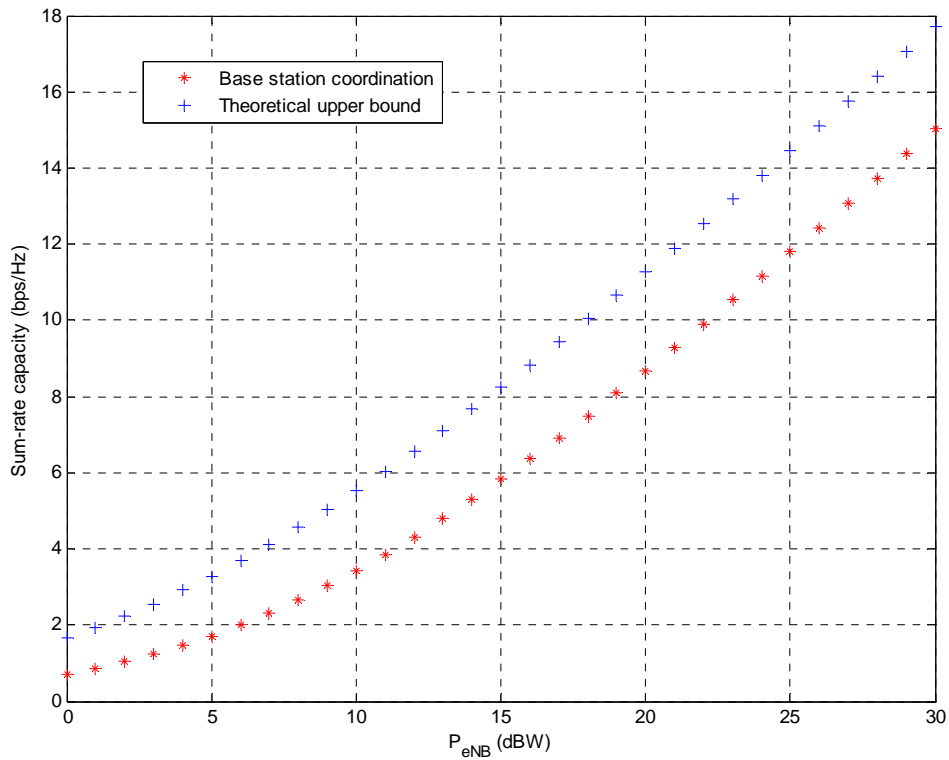


Figure 4.8. Downlink sum-rate capacity versus P_{eNB} : theoretical and zero-forcing base station coordination

Figure 4.8 shows that ZF pre-coding base station coordination cannot reach the dual theoretical sum-rate capacity bound. To achieve the same sum-rate capacity indicated in the theoretical bound, the base station coordination need approximately 4 dB increase in the transmit power, which means ZF is a sub-optimal pre-coding method.

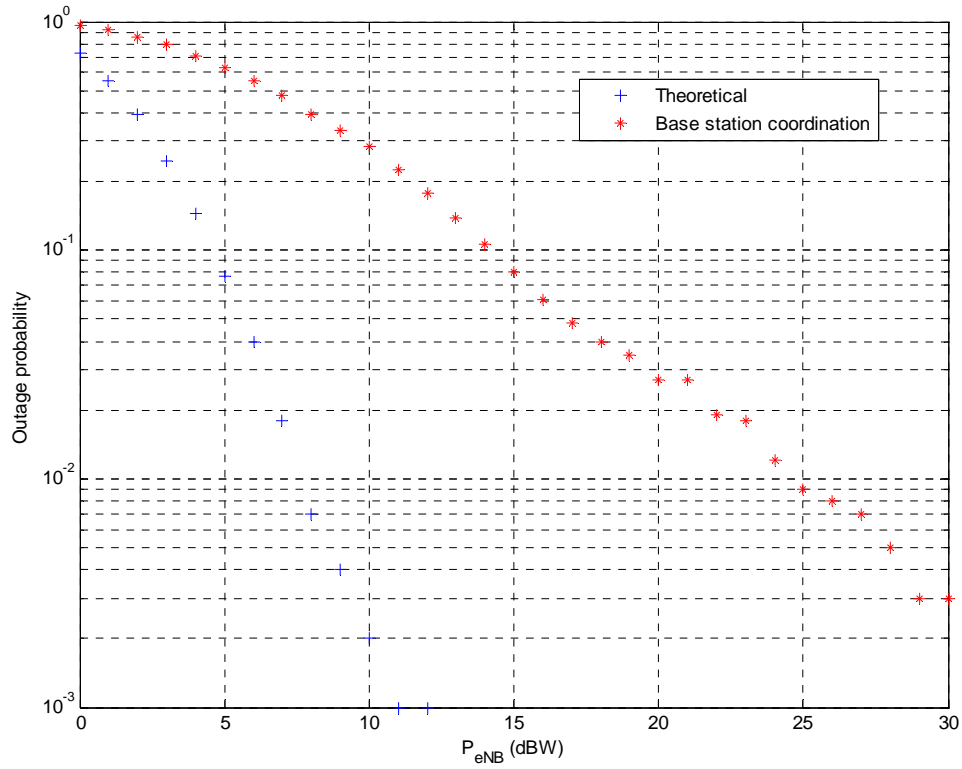


Figure 4.9. Downlink outage probability (at $R=2\text{bps/Hz}$) versus P_{eNB} : theoretical and zero-forcing base station coordination

Figure 4.9 shows that ZF pre-coding base station coordination does not have good outage performance as good as expected in theory because it only cancel the inter-cell interference preliminary but not make use of it for capacity enhancement.

5

THE COMBINATION

It is useful to consider a transmission scheme which combines relaying and base station coordination together, since the relay could enhance the wireless link quality and base station coordination could reduce the inter-cell interference. If it's practical to integrated the two technologies in one, higher spectral efficiencies can be expected. In this chapter, we constraint our analysis in a simple two-cell case in which one eNB and one UE are located in each cell and one RN is located on the board of the two cells.

Section 5.1 introduces the share relaying system. Section 5.2 models the uplink and downlink transmissions in the assumption of combining the shared relaying and base station coordination. Section 5.3 evaluates the capacities achievable in the combination scheme and compares with other three different scenarios.

5.1.Shared relaying

There are different relay architectures for the cellular networks [109][128]. Due to the fact that relaying does not take the inter-cell interference into consideration, we can only assume that transmissions in neighbor cells are time (or frequency) divided. Other than the relay architecture defined in IEEE 802.16j, in which each relay has a single “parent” base station, in this report, we introduce a shared relaying strategy, in which the adjacent eNBs share the same RN, as shown in figure 5.1.

The advantages of shared relaying are more from the deployment point of view. It is obvious that less RNs are needed for completing the task of enhancing the wireless links in several cells.

Similar with symbols and notations in chapter 3 and 4, in this chapter, $h_{AL,k}$ is the channel gain for the AL link from the RN to the k th UE, $h_{DL,mk}$ is the DL channel gain from the m th eNB and the k th UE, and $h_{RL,m}$ is the RL channel gain from the m th eNB to the RN. $x_{eNB,m}$, x_r and $x_{UE,k}$ are the signals transmitted by the m th eNB, the RN and the k th UE, respectively, and the individual power levels are $\mathcal{E}\{|x_{eNB,m}|^2\} = P_{eNB,m}$, $\mathcal{E}\{|x_r|^2\} = P_{RN}$

and $\mathcal{E}\{|x_{UE,k}|^2\} = P_{UE,k}$. The total power allowed in the uplink for the UEs is $P_{eNB} = P_{eNB,1} + P_{eNB,2}$ and maximum power allowed in the downlink for eNBs is $P_{eNB} = P_{eNB,1} + P_{eNB,2}$. $y_{eNB,m}$, y_r and $y_{UE,k}$ are the receive signals at the m th eNB, the RN and the k th UE, respectively. $n_{eNB,m}$, n_r and $n_{UE,k}$ are the noises observed at the m th eNB, the RN and the k th UE, with variances σ^2 , σ_r^2 and σ^2 , respectively. The channel gains in the uplink are assumed to be the conjugate transposes of those in the downlink.

The RN is assumed to be in FDX AF mode in this scheme so that the processing time on the RN can be ignored compared with the pilot time period.

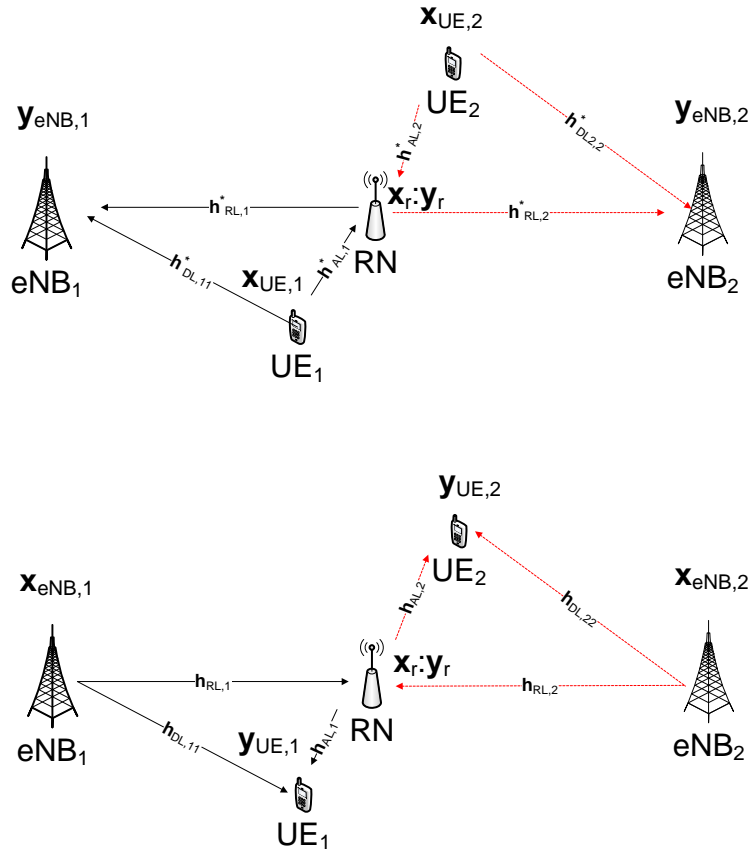


Figure 5.1. Uplink (above) and downlink (below) transmissions with shared relaying

Figure 5.1 shows the transmissions in the uplink and downlink phases for a system with shared relaying, where the black lines denote transmissions in the first time slot and red lines denote transmissions in the second time slot. It is similar with the configuration in section 4.3.1 for the conventional network. The difference is in each of the time slots the transmissions are assisted by a RN which is as modeled in section 3.3.3.

The scheduler allocates one time slot for one cell sequentially, for FDX AF, as indicated in equation (3.24), the sum-rate capacity for the shared relay system in the downlink phase is

$$C_{SR}^{DL} = \frac{1}{2} \left(\log_2 \left(1 + \frac{P_{eNB} |\tilde{h}_1|^2}{\sigma^2 \Lambda_1} \right) + \log_2 \left(1 + \frac{P_{eNB} |\tilde{h}_2|^2}{\sigma^2 \Lambda_2} \right) \right), \quad (5.1)$$

where the subscript SR denotes the shared relaying and the factor $\frac{1}{2}$ is for averaging the rates in two time slots. The other elements are defined as in the section 3.3.3:

$$\begin{cases} \tilde{h}_1 = h_{DL,11} + h_{AL,1} g_{AF,1} h_{RL,1} \\ \tilde{h}_2 = h_{DL,22} + h_{AL,2} g_{AF,2} h_{RL,2} \end{cases}, \quad \begin{cases} \Lambda_1 = 1 + |h_{AL,1}|^2 |g_{AF,1}|^2 \frac{\sigma_r^2}{\sigma^2} \\ \Lambda_2 = 1 + |h_{AL,2}|^2 |g_{AF,2}|^2 \frac{\sigma_r^2}{\sigma^2} \end{cases} \quad \text{and}$$

$$\begin{cases} g_{AF,1} = \sqrt{\frac{P_{RN}}{P_{eNB} |h_{RL,1}|^2 + \sigma_r^2}} \\ g_{AF,2} = \sqrt{\frac{P_{RN}}{P_{eNB} |h_{RL,2}|^2 + \sigma_r^2}} \end{cases}.$$

Similarly, in the uplink phase, the sum-rate capacity is

$$C_{SR}^{UL} = \frac{1}{2} \left(\log_2 \left(1 + \frac{P_{UE} |\tilde{h}_1^{UL}|^2}{\sigma^2 \Lambda_1^{UL}} \right) + \log_2 \left(1 + \frac{P_{UE} |\tilde{h}_2^{UL}|^2}{\sigma^2 \Lambda_2^{UL}} \right) \right), \quad (5.2)$$

$$\text{where } \begin{cases} \tilde{h}_1^{UL} = h_{DL,11}^* + h_{RL,1}^* g_{AF,1}^{UL} h_{AL,1}^* \\ \tilde{h}_2^{UL} = h_{DL,22}^* + h_{RL,2}^* g_{AF,2}^{UL} h_{AL,2}^* \end{cases}, \quad \begin{cases} \Lambda_1^{UL} = 1 + |h_{RL,1}|^2 |g_{AF,1}^{UL}|^2 \frac{\sigma_r^2}{\sigma^2} \\ \Lambda_2^{UL} = 1 + |h_{RL,2}|^2 |g_{AF,2}^{UL}|^2 \frac{\sigma_r^2}{\sigma^2} \end{cases} \quad \text{and}$$

$$\begin{cases} g_{AF,1}^{UL} = \sqrt{\frac{P_{RN}}{P_{UE} |h_{AL,1}^*|^2 + \sigma_r^2}} \\ g_{AF,2}^{UL} = \sqrt{\frac{P_{RN}}{P_{UE} |h_{AL,2}^*|^2 + \sigma_r^2}} \end{cases}.$$

5.2. System model

The system applying the combination of shared relaying and base station coordination is

as shown in figure 5.2.

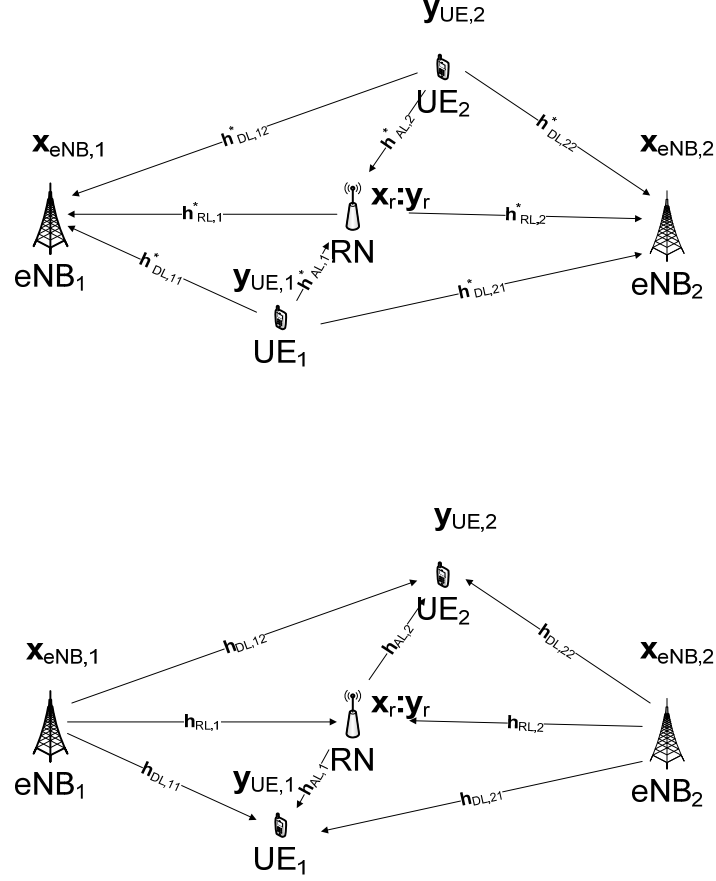


Figure 5.2. Uplink (above) and downlink (below) transmissions in the combination scheme

In the downlink phase, assuming $\mathbf{H} = \begin{pmatrix} h_{DL,11} & h_{DL,21} \\ h_{DL,12} & h_{DL,22} \end{pmatrix}$ is the channel matrix from eNBs

to UEs (DLs) and $\mathbf{h}_r = (h_{RL,1} \quad h_{RL,2})$ is the channel vector from eNBs to RN (RLs), the RN receives

$$\mathbf{y}_r = \mathbf{h}_r \mathbf{x}_{eNB} + n_r, \quad (5.3)$$

where $\mathbf{x}_{eNB} = \begin{pmatrix} x_{eNB,1} \\ x_{eNB,2} \end{pmatrix}$ is the transmit signal vector from the eNBs.

The RN is assumed to be FDX AF, so the forward signal is

$$\mathbf{x}_r = \mathbf{g}_{AF} \mathbf{y}_r, \quad (5.4)$$

according to (3.9), the amplification gain can be expressed by

$$g_{AF} = \sqrt{\frac{P_{RN}}{P_{eNB,1} |h_{RL,1}|^2 + P_{eNB,2} |h_{RL,2}|^2 + \sigma_r^2}}, \quad (5.5)$$

where the denominator denotes the power of receive signal at the RN.

At the k th UE, the receive signal is the addition of the signals from the eNBs and the RN. It can be modeled as

$$\begin{aligned} y_{UE,k} &= \mathbf{h}_k \mathbf{x}_{eNB} + h_{AL,k} x_r + n_{UE,k} \\ &= \underbrace{(\mathbf{h}_k + h_{AL,k} g_{AF} \mathbf{h}_r)}_{\tilde{\mathbf{h}}_k} \mathbf{x}_{eNB} + \underbrace{(h_{AL,k} g_{AF} n_r + n_{UE,k})}_{\tilde{n}_{UE,k}}, \end{aligned} \quad (5.6)$$

where $\mathbf{h}_k = (h_{DL,1k} \quad h_{DL,2k})$ is the channel from eNBs to the k th UE and equal to the k th row of \mathbf{H} . Comparing with the expressions for the base station coordination in (4.16), there are two differences:

1. the channel vector is replaced by $\tilde{\mathbf{h}}_k = \mathbf{h}_k + h_{AL,k} g_{AF} \mathbf{h}_r$;
2. the noise term $\tilde{n}_{UE,k} = h_{AL,k} g_{AF} n_r + n_{UE,k}$ is the amplified noise with power

$$\tilde{N}_{UE,k} = |h_{AL,k}|^2 |g_{AF}|^2 \sigma_r^2 + \sigma^2.$$

As explained in the chapter 4, the system can be treated as a multi-user MIMO system with two distributed transmit antennas and two independent receive antenna. In order to cancel the inter-cell interference, zero-forcing pre-coding is applied at the eNBs, i.e. the condition $\tilde{\mathbf{h}}_k \mathbf{w}_i = 0$, for any $i \neq k$, should be satisfied. \mathbf{w}_i is the i th column of the

pre-coding matrix $\mathbf{W} = \begin{pmatrix} \omega_{11} & \omega_{21} \\ \omega_{12} & \omega_{22} \end{pmatrix}$, which can be found through the procedure

discussed in section 4.3.2 for the base station coordination technology.

Then the sum-rate capacity is

$$C_C^{DL} = \log_2 \left(1 + \frac{|\tilde{\mathbf{h}}_1 \mathbf{w}_1|^2}{\tilde{N}_{UE,1}} \right) + \log_2 \left(1 + \frac{|\tilde{\mathbf{h}}_2 \mathbf{w}_2|^2}{\tilde{N}_{UE,2}} \right), \quad (5.7)$$

where the subscript C denotes the combination transmission scheme, $\tilde{\mathbf{h}}_k$ and $\tilde{N}_{UE,k}$ are as shown in (5.6).

In the uplink phase, assuming $\mathbf{H}^* = \begin{pmatrix} h_{DL,11}^* & h_{DL,12}^* \\ h_{DL,21}^* & h_{DL,22}^* \end{pmatrix}$ is the channel matrix from UEs to eNBs (DLs) and $\mathbf{h}_r^{UL} = (h_{AL,1}^* \quad h_{AL,2}^*)$ is the channel vector from UEs to the RN (ALs), the RN receives

$$y_r^{UL} = \mathbf{h}_r^{UL} \mathbf{x}_{UE} + n_r, \quad (5.8)$$

where $\mathbf{x}_{UE} = \begin{pmatrix} x_{UE,1} \\ x_{UE,2} \end{pmatrix}$ is the transmit signal vector from the UEs.

The RN is assumed to be FDX AF, so the forward signal in the uplink is

$$x_r^{UL} = g_{AF}^{UL} y_r^{UL}, \quad (5.9)$$

according to (3.9), the amplification gain can be expressed by

$$g_{AF}^{UL} = \sqrt{\frac{P_{RN}}{P_{UE,1} |h_{AL,1}|^2 + P_{UE,2} |h_{AL,2}|^2 + \sigma_r^2}}, \quad (5.10)$$

where the denominator denotes the power of receive signal at the RN.

At the eNBs, the received signal vector consists of the signals from the UEs and the RN. It can be modeled as

$$\begin{aligned} \mathbf{y}_{eNB} &= \mathbf{H}^* \mathbf{x}_{eNB} + \begin{pmatrix} h_{RL,1}^* \\ h_{RL,2}^* \end{pmatrix} x_r + \mathbf{n}_{eNB} \\ &= \underbrace{\begin{pmatrix} h_{DL,11}^* + h_{RL,1}^* g_{AF}^{UL} h_{AL,1}^* & h_{DL,12}^* + h_{RL,1}^* g_{AF}^{UL} h_{AL,2}^* \\ h_{DL,21}^* + h_{RL,2}^* g_{AF}^{UL} h_{AL,1}^* & h_{DL,22}^* + h_{RL,2}^* g_{AF}^{UL} h_{AL,2}^* \end{pmatrix}}_{\mathbf{H}^{UL}} \mathbf{x}_{UE} + \underbrace{\begin{pmatrix} h_{RL,1}^* g_{AF}^{UL} n_r + n_{eNB,1} \\ h_{RL,2}^* g_{AF}^{UL} n_r + n_{eNB,2} \end{pmatrix}}_{\mathbf{n}_{eNB}}, \end{aligned} \quad (5.11)$$

where \mathbf{H}^{UL} is the equivalent channel matrix and the noise power at each eNB is then $\tilde{N}_{eNB,m} = |h_{RL,m}^*|^2 |g_{AF}^{UL}|^2 \sigma_r^2 + \sigma^2$. Similar with (3.11) and (3.12), scale the noises power to unit, rewrite (5.11) as

$$\underbrace{\begin{pmatrix} \tilde{N}_{eNB,1}^{-1/2} \mathcal{Y}_{eNB,1} \\ \tilde{N}_{eNB,2}^{-1/2} \mathcal{Y}_{eNB,1} \end{pmatrix}}_{\tilde{\mathbf{y}}_{eNB}} = \underbrace{\begin{pmatrix} \tilde{N}_{eNB,1}^{-1/2} \left(h_{DL,11}^* + h_{RL,1}^* \mathbf{g}_{AF}^{UL} h_{AL,1}^* \right) & \tilde{N}_{eNB,1}^{-1/2} \left(h_{DL,12}^* + h_{RL,1}^* \mathbf{g}_{AF}^{UL} h_{AL,2}^* \right) \\ \tilde{N}_{eNB,2}^{-1/2} \left(h_{DL,21}^* + h_{RL,2}^* \mathbf{g}_{AF}^{UL} h_{AL,1}^* \right) & \tilde{N}_{eNB,2}^{-1/2} \left(h_{DL,22}^* + h_{RL,2}^* \mathbf{g}_{AF}^{UL} h_{AL,2}^* \right) \end{pmatrix}}_{\tilde{\mathbf{H}}^{UL}} \mathbf{x}_{UE} \\
 + \underbrace{\begin{pmatrix} \tilde{N}_{eNB,1}^{-1/2} \left(h_{RL,1}^* \mathbf{g}_{AF}^{UL} \mathbf{n}_r + n_{eNB,1} \right) \\ \tilde{N}_{eNB,2}^{-1/2} \left(h_{RL,2}^* \mathbf{g}_{AF}^{UL} \mathbf{n}_r + n_{eNB,2} \right) \end{pmatrix}}_{\tilde{\mathbf{n}}_{eNB}} \quad , \quad (5.12)$$

where where $\tilde{\mathbf{y}}_{eNB}$, $\tilde{\mathbf{H}}^{UL}$ and $\tilde{\mathbf{n}}_{eNB}$ denote scaled version of receive signal vector, channel matrix and noise vector, respectively.

Since we consider the uplink transmissions are also MIMO multiple accessing, according to equation (4.26), the uplink capacity can be expressed as

$$C_C^{UL} = \log_2 \det \left(\mathbf{I} + \tilde{\mathbf{h}}_1^{UL} P_{UE,1} \tilde{\mathbf{h}}_1^{UL*} + \tilde{\mathbf{h}}_2^{UL} P_{UE,2} \tilde{\mathbf{h}}_2^{UL*} \right), \quad (5.13)$$

where $\tilde{\mathbf{h}}_1^{UL}$ and $\tilde{\mathbf{h}}_2^{UL}$ are the first and second column of the uplink channel matrix $\tilde{\mathbf{H}}^{UL}$ defined in (5.12).

5.3. Performance evaluation

5.3.1. Four scenarios and simulation assumptions

In this section we evaluate the sum-rate capacities for four different scenarios as following:

Scenario 1: Conventional system

The uplink and downlink transmissions are according to section 4.3. 1.

Scenario 2: The system with a shared relay

The uplink and downlink transmissions are according to section 5.1.

Scenario 3: The system with base station coordination

The uplink and downlink transmissions are according to section 4.3.2.

Scenario 4: The system with the combination of shared relaying and base station

coordination

The uplink and downlink transmissions are according to the section 5.2.

According to the WINNER II channel models of path loss described in Appendix A and parameters in table 5.1, simulations are done to show the sum-rate capacities for the four different cases mentioned above.

Table 5.1.Simulation parameters

Number of eNBs	2
Number of RNs	1
Number of UEs	2
Number of antennas on each equipment	1
Height of the eNB	25 (m)
Height of the RN	25 (m)
Height of the UE	1.5 (m)
Maximum total transmit power of eNBs	17 (dBW)
Maximum transmit power of the RN	14 (dBW)
Maximum total transmit power of UEs	5 (dBW)
eNB-RN channel model	WINNER II B5a
eNB-UE channel model	WINNER II C2 NLOS
RN-UE channel model	WINNER II C2 NLOS
Number of realizations	1000
Cell radius	876 (m)
Noise power	-144 (dBW)
Carrier frequency	2 (GHz)
Distance between the eNB and the UE in the same cell	700 (m)
Distance between the eNB and the UE in the different cell	1052 (m)
Distance between the RN and the UE	176 (m)

Denote a as the factor of attenuation caused by the path loss and shadowing, which can be calculated through the models described in Appendix A. Note that a is varying for different links DLs, RLs and ALs. The channel gains of RLs and ALs are all assumed to be complex Gaussian $\sim a \times \mathcal{CN}(0,1)$, which indicates the Rayleigh fading environment. The small-scale fading on the DLs is ignored due to the strong LOS transmission. The noises in the network are assumed to be additive and with variances $\sigma^2 = \sigma_r^2 = -144$ (dBW). For statistic channel coefficients, the expected capacity is the average of sum-rate capacities in each channel realization (1000 times), which can be calculated by equation (4.17), (4.18), (4.24), (4.27), (5.1), (5.2), (5.7) and (5.13) accordingly. For simplicity, the power levels are assumed to be same for all the eNBs or UEs, i.e. $P_{eNB,1} = P_{eNB,2} = \frac{1}{2} P_{eNB}$ and $P_{UE,1} = P_{UE,2} = \frac{1}{2} P_{UE}$.

5.3.2. Numerical results

First we evaluate the sum-rate capacities with the changes in eNBs (or UEs in the uplink phase) transmit power P_{eNB} (P_{UE} in the uplink phase). The RN transmit power P_{RN} is set as 50% of P_{eNB} accordingly.

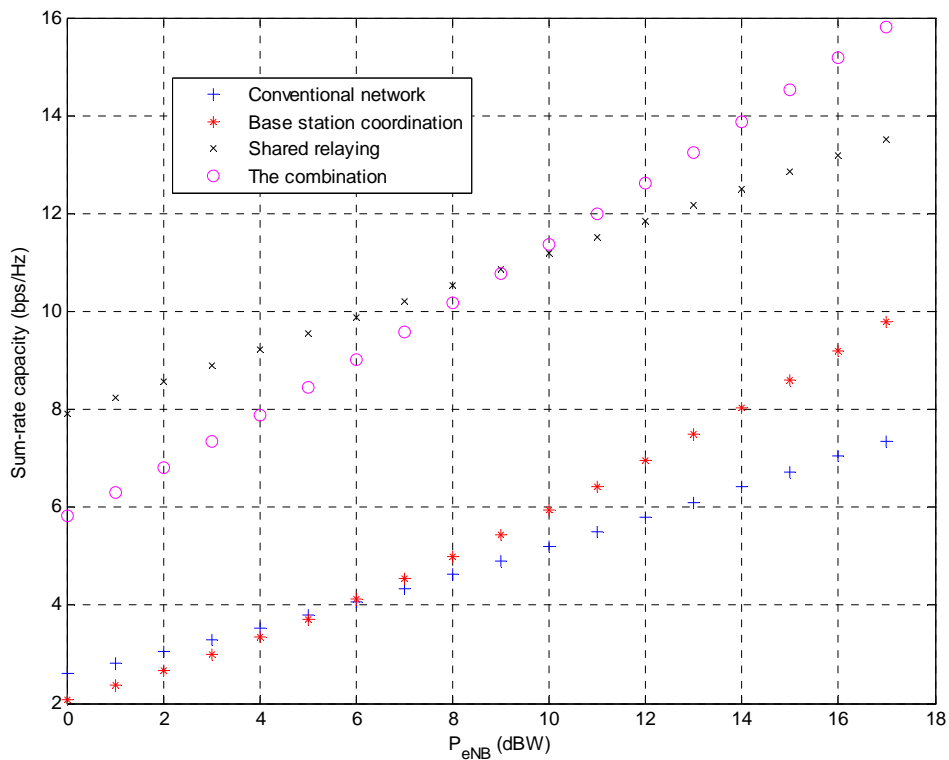


Figure 5.3. Downlink sum-rate capacity versus P_{eNB} : four Scenarios

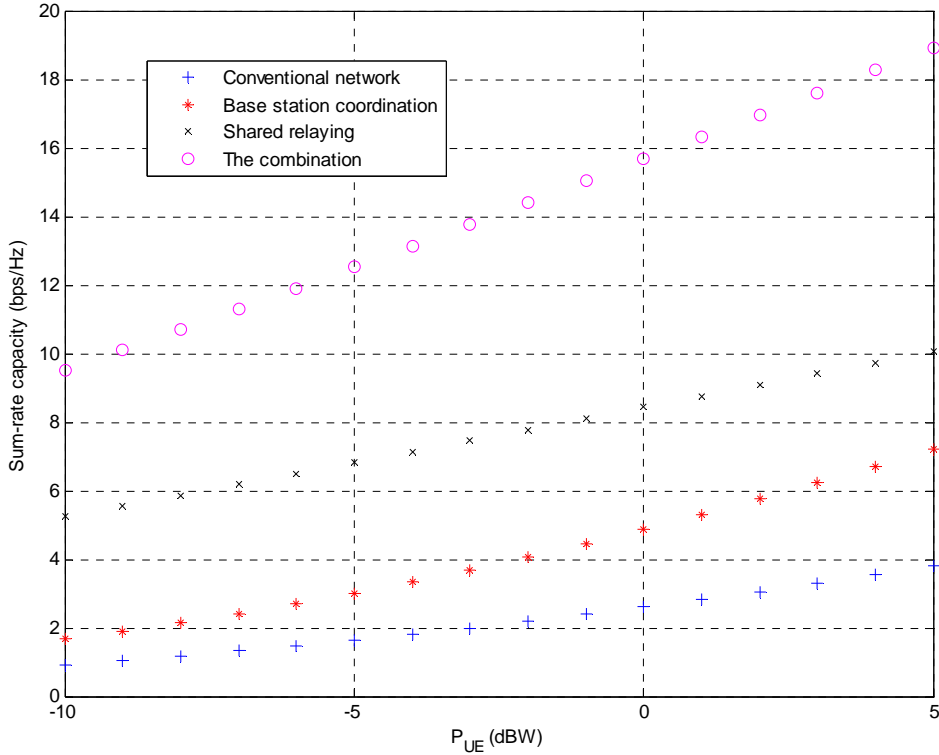

 Figure 5.4. Uplink sum-rate capacity versus P_{UE} : four Scenarios

Figure 5.3 and 5.4 show the relationships between sum-rate capacities and eNB transmit antenna power in the downlink phase and UE transmit antenna power in the uplink phase, respectively. Generally the sum rates are increasing with the antennas power, since higher transmitted power leads to higher SNR. In the downlink, because of the sub-optimal nature of zero-forcing pre-coding, the combination of shared relaying and base station coordination outperforms the others at high transmit power (> 9 dBW) and the shared relaying is the best choice when transmit power of eNB is lower than 9 dBW. This results also implies the main contribution in the performance improvement is done by the RN. The close distance between the RN and UE causes this consequence. For a simple calculation, following the parameters set in table 5.1, in the downlink phase, when $P_{eNB} = 0$ dBW, $P_{RN} = \frac{1}{2} P_{eNB} = -3$ dBW a typical receive SNR of the DL at the UE is $\frac{P_{eNB}}{\sigma^2} |h_{DL,11}|^2 \approx 15.5dB$, and a typical receive SNR of the AL at the UE is $\frac{P_{RN}}{\sigma^2} |h_{AL,1}|^2 \approx 36.5dB$. So that the transmissions of the RN dominate the system performance. In the uplink, the achievable sum-rates capacities follow the order

$$C_C^{UL} > C_{SR}^{UL} > C_{BSC}^{UL} > C_{CON}^{UL}.$$

Next we fix the eNBs (UEs) power as maximum and change P_{RN} to check the benefits obtained from the RN.

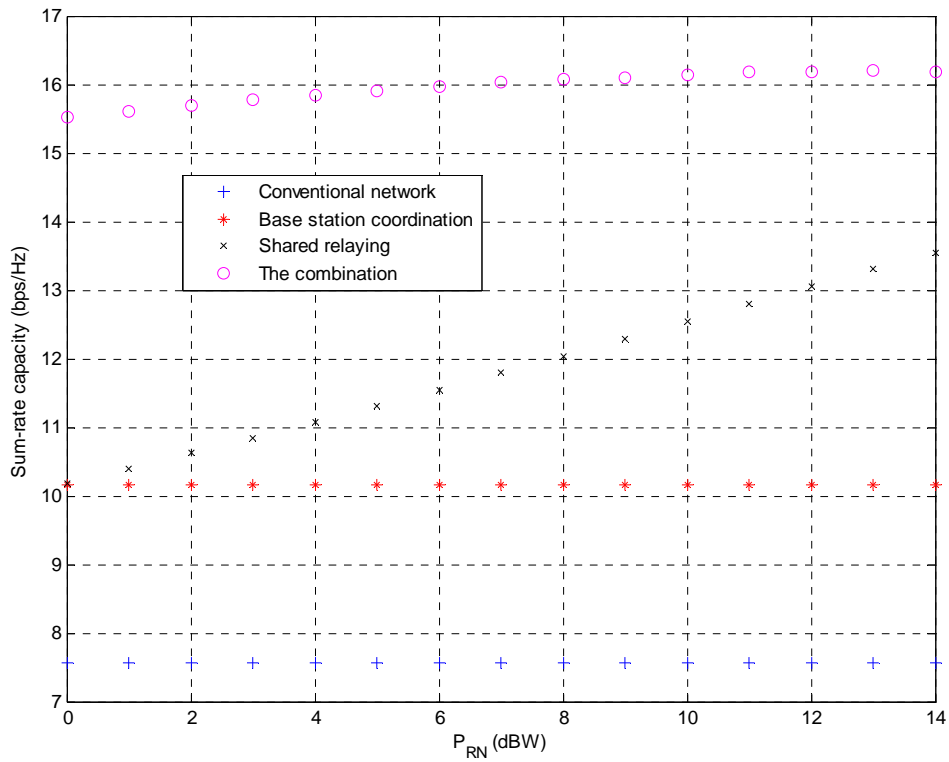


Figure 5.5. Downlink sum-rate capacity versus P_{RN} : four Scenarios

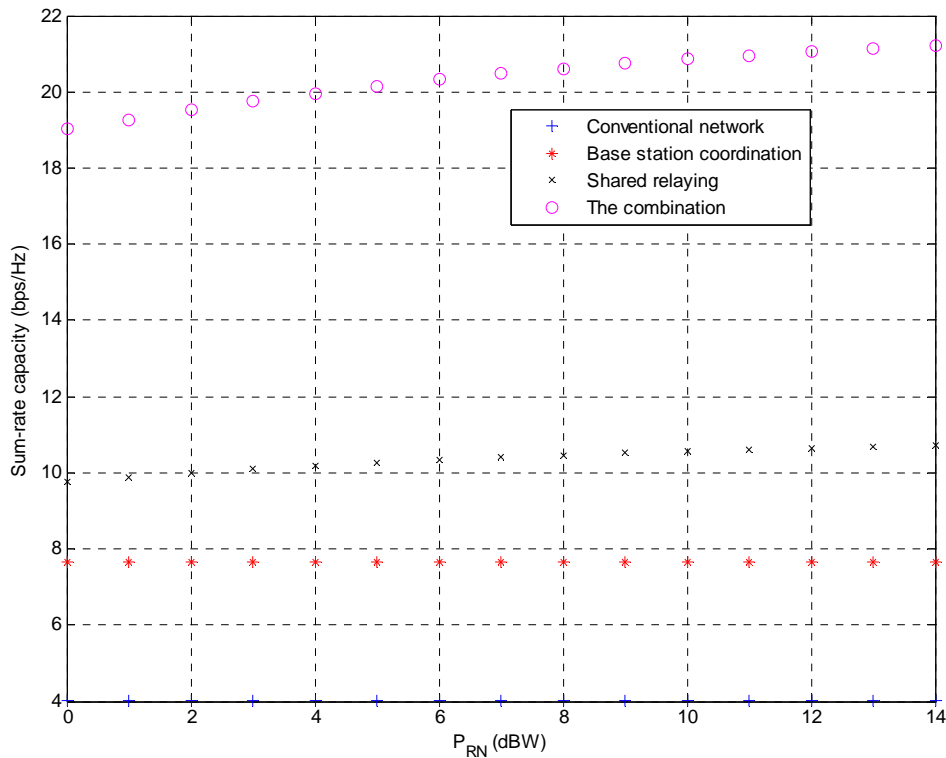


Figure 5.6. Uplink sum-rate capacity versus P_{RN} : four Scenarios

Figure 5.5 and 5.6 show how sum-rate capacities change with the increasing of RN transmit power. The performances of convention system and coordinated eNBs stay unchanged since there's no RN deployed in these two cases. We can see that in the downlink phase, when the power of RN increases from 0 dBW to 14 dBW, the capacity of the combination case grows with 0.5 bps/Hz while the capacity of share relaying system increases with 3.5 bps/Hz. In the uplink phase, for 14dB increase in power of the RN, the capacity of the combination case grows with 2 bps/Hz while the capacity of share relaying system increases with 1 bps/Hz.

Assume that the eNBs, the RN and UEs are aligned in a straight line, which means if the distance between the RN and UE_1 is d_1 (originally in table 5.1, $d_1 = 176$ (m)), then the distance between UE and eNB_1 is $876 - d_1$ (m) and the distance between UE and eNB_2 is $876 + d_1$ (m). Then we show the influences of UEs' locations to the system sum-rate capacities. Set P_{eNB} and P_{RN} at the maximum and varying the distances between the RN and UEs d_1 to draw a 3-D surface.

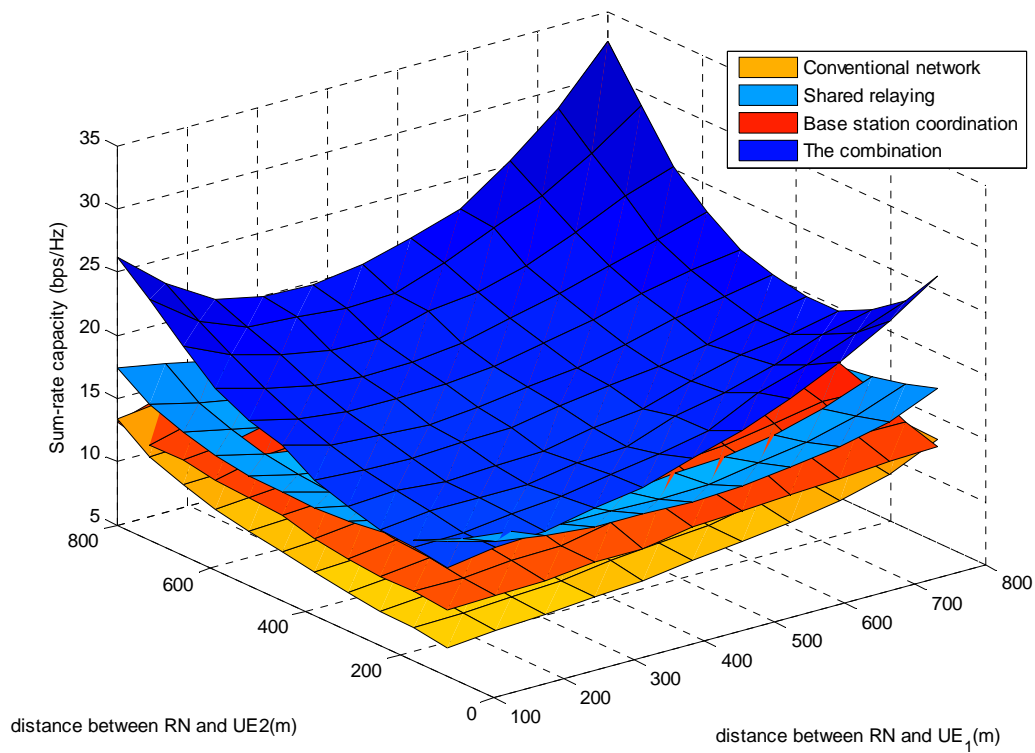


Figure 5.7. Downlink sum-rate capacity versus distance apart from RN: four scenarios

Figure 5.7 shows the influences of UEs' locations in the downlink transmissions. With the highest transmitted power levels on both RN and eNBs, we change the positions of UEs along a path from RN to eNB. The combination of shared relaying with base station coordination outperforms the others in all the covered area.

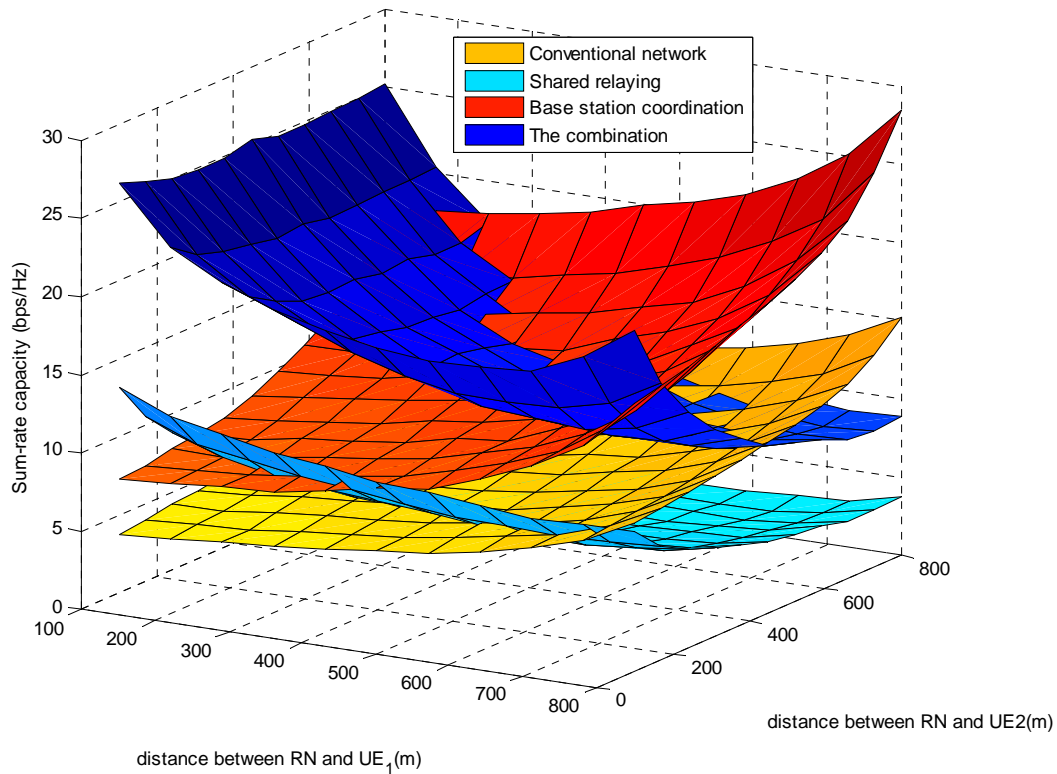


Figure 5.8. Uplink sum-rate capacity versus distance apart from RN: four scenarios

Figure 5.8 shows the influences of UEs' locations in the uplink phase. With the highest transmitted power levels on both RN and eNBs, we change the positions of UEs along a path from RN to eNB. The combination of shared relay with base station coordination outperforms the others in the region where the UEs are close to the RN and the pure base station coordination seems to be the best choice for the case that all the UE are located near the their 'parent' eNBs. When the UEs are far away from the RN, the useful signal receive at the RN from UEs is very weak. Since the RN is FDX AF, the signal it forwards will contain a large proportion of noises. That is the reason why the shared RN plays a negative role for the system capacity in the uplink when the UEs are not at the cell board.

From figures 5.3-5.8, we can conclude that the combination of techniques is feasible and efficient methods to enhance the cell edge performance. For the cell-edge UEs, they mainly benefit from the assistant of the RN. However, if all the UEs are close to the eNBs, the combination scheme may not have the best performance. The control point should do the scheduling task based on the channel state information and decide the most suitable transmission scheme for the specific users at the specific positions.

6

CONCLUSION AND FUTURE WORK

In this report, we investigate relaying and base station coordination technologies and their combination in LTE-Advanced networks with the purpose of improving the cell-edge multi-user performance. We divide the task into three main parts, which are discussed in chapter 3, 4 and 5 respectively.

Firstly, we analyze the relaying technology. With the knowledge that relaying could enhance the wireless links, we examine the differences between the HDX/FDX work mode and AF/DF forward strategies. FDX relaying reaches nearly twice of the performance of the HDX relaying and DF relaying is limited by the quality of relay link because the rate of the first time slot should satisfy the requirement of the reliable decoding procedure on the RN. If the RL is ideal, DF relaying outperforms AF relaying in a capacity point-of-view because it does not forward noises in the network.

Secondly, we evaluate the base station coordination technology. With multi-cell processing, the adjacent eNBs can form a virtual antenna array and then the system can then be model as MIMO MAC and MIMO BC in uplink and downlink phases respectively. With the tools provided by the multi-user information theory, we can calculate the theoretical bound of multi-user MIMO sum-rate capacity. Zero-forcing pre-coding is chosen to realize multi-user transmissions in the downlink phase in the base station coordination scheme discussed in this report. In an application of these theories in a two-cell system, inter-cell interference is perfectly eliminated and the capacity enhancement compared with the conventional system is proven in the case of relatively high SNR.

Finally, a combination scheme is proposed based on the idea that enhancing the wireless link and reducing the inter-cell interference could be done concurrently. A shared relay node is chosen as the relay architecture for the reason that less RN deployments are required in the network. Numerical results show that this transmission scheme can enable the simultaneous transmissions to multiple users in different cells and gain higher sum-rate capacity than those systems applying relaying or base station coordination alone. So that it is a good solution for improving the cell-edge multi-user performance.

Future works still need to be done in the following areas:

1. The feedback and estimation of the channel state information. Throughout the report, the channel status information (or the distribution) is assumed perfectly known at least at the eNBs. However, in a practical system, the methods of acquiring the real-time channel status information are difficult to realize since the wireless links vary with time and the accurate estimations of the channel status are quite important.
2. The synchronization in each frame. Since there are plenty of co operations among the eNBs, RNs and even UEs, the synchronizations of signals are of importance to the success of transmissions.
3. The scheduling algorithm for better resources allocation over a large number of RBs. The scheduler will not only decide the pre- and post- processing but also be involved with selection of RBs, the fairness of the achievable rates of multiple users, etc.
4. The better pre-coding design which can be adapted in a large scale network with large number of cells. We can see the zero-forcing pre-coding is sub-optimal even for a simple 2×2 channel matrix. In reality, the design will face challenges like the rank deficient matrix, correlated antennas, etc.

Appendices

Appendix A: WINNER II channel path loss models [124]

Channel state information is very important, particularly for coordinated eNBs to decide their pre-coding weights matrix, and its time-variant nature makes the measurements even more complicated. In proposed drafts for LTE-Advanced, the channel state information is obtained from some specific reference signaling. In this report the perfect channel state information is assumed at the eNBs, but good models are still needed to make the simulation more practical. Here two types in WINNER II - Wireless World Initiative New Radio model II, scenario B5a and scenario C2 Non-Line-Of-Sight (NLOS), are selected to model the transmissions from eNB to RN and from eNB/RN to UE, respectively.

The typical path loss model in WINNER II is

$$PL = A \log_{10}(d) + B + C \log_{10}\left(\frac{f_c}{5}\right) + X,$$

where d is the distance between the transmitter and the receiver, f_c is the carrier frequency, the fitting parameter A includes the path-loss exponent, parameter B is the intercept, parameter C describes the path loss frequency dependence, and X is an optional, environment-specific term. The shadow fading is assumed to follow zero-mean Normal Distribution with standard derivation σ .

The eNB to RN channel is chosen following scenario B5a where the connection is almost like in free space and signals can be assumed to consist of a strong LOS signal and single bounce reflection,

$$PL = 23.5 \log_{10}(d) + 42.5 + 20 \log_{10}\left(\frac{f_c}{5}\right),$$

with shadow fading standard derivation $\sigma = 4$.

The channel from eNB/RN to the UE is assumed to be in scenario C2 Non-Line-Of-Sight, which is a typical urban macro-cell that UE is located outdoors at street level and fixed eNB clearly above surrounding building heights. NLOS is a common case, since street level is often reached by a single diffraction over the rooftop,

$$PL = (44.9 - 6.55 \log_{10}(H_{BS})) \log_{10}(d) + 34.46 + 5.83 \log_{10}(H_{BS}) + 23 \log_{10}\left(\frac{f_c}{5}\right),$$

with shadow fading standard derivation $\sigma = 8$, where H_{BS} is the height of the base station (eNB) antenna.

Reference

- [1] 3GPP TS21.101, “Overview of 3GPP Release 10; Summary of all Release 10 Features (Release 10)”, April 2011, http://www.3gpp.org/ftp/Information/WORK_PLAN/Description_Releases/
- [2] IEEE 802.16 Broadband Wireless Access Working Group, “Channel Models for Fixed Wireless Applications”, July 2001, http://www.ieee802.org/16/tg3/contrib/802163c-01_29r4.pdf
- [3] IEEE 802.16 Broadband Wireless Access Working Group, “Multi-hop Relay System Evaluation Methodology (Channel Model and Performance Metric)”, Feb. 2007, http://www.ieee802.org/16/relay/docs/80216j-06_013r3.pdf
- [4] H. Suzuki, et al., “A Booster Configuration with Adaptive Reduction of Transmitter-Receiver Antenna Coupling for Pager Systems”, in IEEE VTC 1999 fall, vol.3, pp.1516-1520, 1999
- [5] H. Boche and M. Schubert, “A General Duality Theory for Uplink and Downlink Beamforming”, in IEEE VTC 2002, vol.1, pp.87-91,2002
- [6] J. Lee and H. Yanikomeroglu, “A Novel Architecture for Multi-hop WiMAX Systems: Shared Relay Segmentation”, in IEEE WCNC 2010, pp.1, 2010
- [7] C. Hoymann et al., “A Self-backhauling Solution for LTE-Advanced”, in WWRF 21-WG4 Stockholm, Sweden, 2008
- [8] Q. Zhang and D. Liu, “A simple capacity formula for correlated diversity Rician fading channels”, in IEEE Communications Letter, vol.6, issue 11, pp. 481-483, 2002
- [9] J.P. Kermoal et al., “A Stochastic MIMO Radio Channel Model With Experimental Validation”, in IEEE journal on Selected Areas in Communications, vol.20, issue 6, pp.1211-1226, 2002
- [10] H. Hamazumi et al., “A Study of a Loop Interference Canceller for the Relay Stations in an SFN for Digital Terrestrial Broadcasting”, in IEEE GLOBECOM 2000, vol.1, pp.167-171, 2000
- [11] R. Kwan and C. Leung, “A Survey of Scheduling and Interference Mitigation in LTE”, in Journal of Electrical and Computer Engineering, vol. 2010, pp. 1–10, 2010
- [12] G. Piro et al., “A Two-level Scheduling Algorithm for QoS Support in the Downlink of LTE cellular networks”, in 2010 European Wireless Conference, pp.246, 2010
- [13] B.M. Hochwald, C.B. Peel and A.L. Swindlehurst, “A vector-perturbation technique for near-capacity multi-antenna multiuser communication: Part I, channel inversion and

REFERENCE

- regularization”, in IEEE Transactions on Communications, vol.53, issue 1, pp.195-202, 2005
- [14] B.M. Hochwald, C.B. Peel and A.L. Swindlehurst, “A vector-perturbation technique for near-capacity multi-antenna multi-user communication: Part II, Perturbation”, in IEEE Transactions on Communications, vol.53, issue 3, pp.537-544, 2005
- [15] R. Nikjah and N.C. Beaulieu, “Achievable Rates and Fairness in Rateless Coded Decode-and-Forward Half-Duplex and Full-Duplex Opportunistic Relaying”, in IEEE ICC 2008, pp.3701-3707,2008
- [16] M. Pischella and J.C. Belfiore, “Achieving a Frequency Reuse Factor of 1 in OFDMA Cellular Networks with Cooperative Communications”, in IEEE VTC 2008 spring, pp.653-657, 2008
- [17] C. Bae and D. Cho, “Adaptive resource allocation based on channel information in multihop OFDM systems”, in IEEE VTC 2006 fall, pp.1-5, 2006
- [18] B. Karakaya, H. Arslan, and H. A. Curpan, “An adaptive channel interpolator based on Kalman filter for LTE uplink in high Doppler spread environments,” in EURASIP Journal on Wireless Communication And Networking, vol. 2009, 2009
- [19] R. Schoenen, R. Halfmann and B.H. Walke, “An FDD Multihop Cellular Network for 3GPP-LTE”, IEEE VTC 2008 spring, pp.1990-1994, 2008
- [20] X. Fan, S. Chen and X. Zhang, “An Inter-Cell Interference Coordination Technique Based on Users’ Ratio and Multi-Level Frequency Allocations”, in International Conference Wicom 2007, pp.799-802, 2007
- [21] D.J. Love et al., “An Overview of Limited Feedback in Wireless Communication Systems”, in IEEE journal on Selected Areas in Communications, vol.26, issue 8, pp.1341-1365, 2008
- [22] U. Erez, S. Shamai and R. Zamir, “Capacity and lattice strategies for canceling known interference”, in IEEE Transactions on Information Theory, vol.51, issue 11, pp.3820-3833, 2005
- [23] L. Li and A.J. Goldsmith, “Capacity and Optimal Resource Allocation for Fading Broadcast Channels: Part I Ergodic Capacity”, in IEEE Transactions on Information Theory, vol.47, issue 3, pp.1083-1102, 2001
- [24] L. Li and A.J. Goldsmith, “Capacity and Optimal Resource Allocation for Fading Broadcast Channels: Part II Outage Capacity”, in IEEE Transactions on Information Theory, vol.47, issue 3, pp.1103-1127, 2001
- [25] A.J. Goldsmith and P.P. Varaiya, “Capacity of fading channel with Channel Side Information”, in

- IEEE Transactions on Information Theory, vol.43, issue 6, pp.1986-1992, 1997
- [26] A.J. Goldsmith et al., "Capacity Limits of MIMO Channels", in IEEE journal on Selected Areas in Communications, vol.21, issue 5, pp.684-702, 2003
- [27] T.L. Marzetta and B.M. Hochwald, "Capacity of a mobile multiple-antenna communication link in Rayleigh flat fading", in IEEE Transactions on Information Theory, vol.45, issue 1, pp.139-157, 1999
- [28] O. Simeone et al., "Capacity of linear two-hop mesh networks with rate splitting, decode-and-forward relaying and cooperation," in Proceedings of the Allerton Conference, Monticello, Ill, USA, September 2007
- [29] M. Kang and M.S. Alouini, "Capacity of MIMO Rician Channels", in IEEE Transactions on Information Theory, vol.5, issue 1, pp.112-122, 2006
- [30] E. Telatar, "Capacity of Multi-antenna Gaussian Channels", in European transactions on telecommunications, vol.10, issue 8, pp.585-595, 1999
- [31] T. Cover and A.E. Gamal, "Capacity Theorems for the Relay Channel", in IEEE Transactions on Information Theory, vol.25, issue 5, pp.572-584, 1979
- [32] O. Simeone et al., "Cellular networks with Full-Duplex Amplify-and-Forward Relaying and Cooperative Base-Stations", in Proceedings of the IEEE International Symposium on Information Theory, pp. 16-20, June 2007
- [33] O. Simeone et al., "Cellular networks with Full-Duplex Compress-and-Forward Relaying and Cooperative Base Stations", in Proceedings of the IEEE International Symposium on Information Theory, pp. 2086-2090, July 2008
- [34] O. Somekh et al, "Cellular networks with Non-Regenerative Relaying and Cooperative Base Stations", in IEEE Transactions on Wireless Communications, vol.9, issue 8, pp.2654-2663, 2010
- [35] S. Brueck, "Centralized scheduling for joint transmission coordinated multi-point in LTE-Advanced", in 2010 International ITG Workshop on Smart Antennas, pp.177-184, 2010
- [36] I. Hammerstrom, M. Kuhn and A. Wittneben, "Channel Adaptive Scheduling for Cooperative Relay Networks", IEEE VTC 2004 fall, vol.4, pp.2784-2788, 2004
- [37] R. Schoenen, D. Bultmann and Z. Xu, "Channel quality indication for adaptive resource scheduling in Multihop OFDMA systems", in European Wireless Conference, pp.58-62, 2009
- [38] N. Kolehmainen et al., "Channel Quality Indication Reporting Schemes for UTRAN Long Term

REFERENCE

- Evolution Downlink”, in IEEE VTC 2008 spring, pp.2522-2526, 2008
- [39] L. Ruiz de Temino, “Channel-Aware Scheduling Algorithms for SC-FDMA in LTE Uplink”, in IEEE International Symposium on PIMRC 2008, pp.1-6, 2008
- [40] T. Riihonen, S. Werner and R. Wichman, “Comparison of Full-Duplex and Half-Duplex Modes with a Fixed Amplify-and-Forward Relay”, in IEEE WCNC 2009, pp.1-5, 2009
- [41] T. Ratnarajah, R. Vaillancourt and M. Alvo, “Complex Random Matrices and Rician Channel Capacity”, in *Probl. Inform. Transm.*, vol. 41, no. 1, pp. 1–22, Jan. 2005
- [42] J.N. Laneman, D.N.C. Tse and G.W. Wornell, “Cooperative diversity in wireless networks-efficient protocols and outage behavior”, in *IEEE Transactions on Information Theory*, vol.50, issue 12, pp.3062-3080, 2004
- [43] E. Björnson et al., “Cooperative Multi-cell Pre-coding: Rate Region Characterization and Distributed Strategies With Instantaneous and Statistical CSI”, in *IEEE Transactions on Signal Processing*, vol.58, issue 8, pp.4298-4310, 2010
- [44] Y. Fan et al., “Cooperative Multiplexing: Toward Higher Spectral Efficiency in Multiple-Antenna Relay Networks”, in *IEEE Transactions on Information Theory*, vol.55, issue 9, pp.3909-3926, 2009
- [45] G. Kramer, M. Gastpar and P. Gupta, “Cooperative Strategies and Capacity Theorems for Relay Networks”, in *IEEE Transactions on Information Theory*, vol.51, issue 9, pp.3037-3063, 2005
- [46] Yan Zhang , Hsiao-Hwa Chen , Mohsen Guizani, “Cooperative Wireless Communications”, Auerbach Publications, Boston, MA, 2009
- [47] G.J. Foschini, K. Karakayali and R.A. Valenzuela, “Coordinating multiple antenna cellular networks to achieve enormous spectral efficiency”, in *IEE Proceeding of Communications*, vol.153, issue 4, pp.548-555, 2006
- [48] J. Li, Z. Hu and Y. Wang, “DF/AF cooperative relay in LTE-A”, in IEEE VTC 2010 spring, pp.1-5, 2010
- [49] N. Jindal and A. Goldsmith, “Dirty-paper coding versus TDMA for MIMO Broadcast channels”, in *IEEE Transactions on Information Theory*, vol.51, issue 5, pp.1783-1794, 2005
- [50] L. Zheng and D.N.C. Tse, “Diversity and Multiplexing: A Fundamental Tradeoff in Multiple-Antenna Channels”, in *IEEE Transactions on Information Theory*, vol.49, issue 5, pp.1073-1096, 2003

- [51] P. Komulainen, "Downlink assisted uplink zero forcing for TDD multiuser MIMO systems", in IEEE WCNC 2009, pp.1-6, 2009
- [52] B. Sadiq, R. Madan, and A. Sampath, "Downlink scheduling for multiclass traffic in LTE," in EURASIP J. Wireless Commun. Netw., vol. 2009, pp. 1–18, Aug. 2009
- [53] P. Kela, "Dynamic Packet Scheduling Performance in UTRA Long Term Evolution Downlink", in ISWPC 2008, pp.308-313, 2008
- [54] O. Teyeb et al., "Dynamic relaying in 3GPP LTE-advanced networks", in EURASIP Journal on Wireless Communication And Networking, vol. 2009, no.6, 2009
- [55] B. Mathias et al., "Dynamic resource allocation in OFDM systems, an overview of cross-layer optimization principles and techniques", in IEEE Network, vol.21, issue 1, pp.53-59, 2007
- [56] T. Beniero et al., "Effect of Relaying on Coverage in 3GPP LTE-Advanced", in IEEE VTC 2009 spring, pp.1-5, 2009
- [57] T.M. Cover, and J.A. Thomas, "Elements of information theory", Wiley, New York, 1991
- [58] S. Shamai and B.M. Zaidel, "Enhancing the Cellular Downlink Capacity via Co-processing at the Transmitting End", in IEEE VTC 2001 spring, vol.3, pp.1745-1749, 2001
- [59] W.C.Y. Lee, "Estimate of Channel Capacity in Rayleigh Fading Environment", in IEEE Transactions on Vehicular Technology, vol.39, issue 3, pp.187-189, 1990
- [60] R.U. Nabar, H. Bolcskei and F.W. Kneubuhler, "Fading relay channels performance limits and space-time signal design", in IEEE journal on Selected Areas in Communications, vol.22, issue 6, pp.1099-1109, 2004
- [61] I. Maric and R.D. Yates, "Forwarding strategies for Gaussian parallel-relay network", in ISIT 2004 Proceedings, pp.269, 2004
- [62] Y. Zhao et al., "Fractional frequency reuse schemes and performance evaluation for OFDMA multi-hop cellular networks", in International Conference on TridentCom 2009, pp.1-5, 2009
- [63] A. Simonsson, "Frequency Reuse and Inter-cell Interference Co-ordination in E-UTRA", IEEE VTC 2007 spring, pp.3091-3095, 2007
- [64] J. Lee and O. Shin, "Full-Duplex Relay based on Zero-Forcing beam forming", IEICE TRANSACTIONS on Communications, vol.E94-B, no.4, pp.978-985, 2011
- [65] R. Knopp and P.A. Humblet, "Information capacity and power control in single-cell multiuser

REFERENCE

- communications”, in IEEE ICC’95 Seattle, ‘Gateway to Globalization’, vol.1, pp.331-335, 1995
- [66] M.R. Souryal, B.R. Vojcic and R.L. Pickholtz, “Information efficiency of multihop packet radio networks with channel-adaptive routing”, in IEEE journal on Selected Areas in Communications, vol.23, issue 1, pp.40-50, 2005
- [67] X. Zhang et al., “Inter-cell Interference Coordination Based on Softer Frequency Reuse in OFDMA Cellular networks”, 2008 International Conference on Neural Networks and Signal Processing, pp.270-275, 2008
- [68] M. Schubert and H. Boche, “Iterative Multiuser Uplink and Downlink Beam forming Under SINR Constraints”, IEEE Transactions on Signal Processing, vol.53, issue 7, pp.2324-2334, 2005
- [69] L. Cottatellucci, T. Chan and N. Fawaz, “Large System Design and Analysis of Protocols for Decode-Forward Relay Networks”, in International Symposium on WiOPT 2008, pp.591-596, 2008
- [70] A.G. Gotsis, D. Komnakos and P. Constatninou, “Linear Modeling and Performance Evaluation of Resource Allocation and User Scheduling for LTE-like OFDMA networks”, in ISWCS 2009, pp.196-200, 2009
- [71] E. Yaacoub, H. Al-Asadi and Z. Dawy, “Low Complexity Scheduling Algorithms for the LTE Uplink”, In ISCC 2009, pp.266-270, 2009
- [72] T.E. Kolding, F. Frederiksen and A. Pokhariyal, “Low-Bandwidth Channel Quality Indication for OFDMA Frequency Domain Packet Scheduling”, in ISWCS’06, pp.282-286, 2006
- [73] F. Khan, “LTE for 4G Mobile Broadband”, New York, Cambridge University Press, 2009
- [74] R. Schoenen, R. Halfmann and B.H. Walke, “MAC Performance of a 3GPP-LTE Multihop Cellular Network”, in IEEE ICC 2008, pp.4819-4824, 2008
- [75] K. Haneda et al., “Measurement of Loop-Back Interference Channels for Outdoor-to-Indoor Full-Duplex Radio Relays”, in 2010 Proceedings of the fourth EuCAP, pp.1-5, 2010
- [76] N. Jindal, “MIMO Broadcast Channels with Finite Rate Feedback”, in IEEE Transactions on Information Theory, vol.52, issue 11, pp.5045-5060, 2006
- [77] Y. Fan and J. Thompson, “MIMO Configurations for Relay Channels Theory and Practice”, in IEEE transactions on Wireless Communications, vol.6, issue 5, pp.1774-1786, 2007
- [78] J. Lee and J.-K. Han et al., “MIMO technologies in 3GPP LTE and LTE-advanced,” in EURASIP J. Wireless Communications and Network., vol. 2009, 2009.

-
- [79] E. Biglieri , R. Calderbank , A. Constantinides , A. Goldsmith , A. Paulraj , H. Vincent Poor, “MIMO Wireless Communications”, Cambridge University Press, New York, NY, 2007
- [80] M. Cao et al., “Modeling and Performance Analysis of the Distributed Scheduler in IEEE 802.16 Mesh Mode,” Proc. 6th ACM Int’l. Symp. Mobile Ad Hoc Networking and Comp., Urbana-Champaign, IL, 2005, pp. 78–89
- [81] T. Endeshaw, B.K. Chalise and L. Vandendorpe, “MSE uplink-downlink duality of MIMO systems under imperfect CSI”, in IEEE International Workshop on CAMSAP 2009, pp.384-387, 2009
- [82] D. Gesbert et al., “Multi-Cell MIMO Cooperative Networks: A New Look at Interference”, in IEEE journal on Selected Areas in Communications, vol.28, issue 9, pp.1380-1408, 2010
- [83] J. Yang and D. Kim, “Multi-cell uplink-downlink beam forming throughput duality based on Lagrangian duality with per-base station power constraints”, in IEEE Communications Letters, vol.12, issue 4, pp.277-279, 2008
- [84] A. Shadmand and S-B, Mohammad, “Multi-user Time-Frequency Downlink Scheduling and Resource Allocation for LTE Cellular networks”, in IEEE WCNC 2010, pp.1-6, 2010
- [85] K. Zhang et al., “Multihop cellular networks toward LTE-advanced”, in IEEE Vehicular Technology Magazine, vol.4, issue 3, pp.40-47, 2009
- [86] O. Oyman, N.J. Laneman and S. Sandhu, “Multihop Relaying for Broadband for Wireless Mesh Network: From Theory to Practice”, in IEEE Communications Magazine, vol.45, issue 11, pp.116-122, 2007
- [87] K. Karakayali, G.J. Foschini and R.A. Valenzuela, “Network coordination for spectrally efficient communications in cellular networks”, in IEEE Wireless Communications, vol.13, issue 4, pp.56-61, 2006
- [88] M. Salem et al., “Nomadic Relay-directed Joint Power and Subchannel Allocation in OFDMA-based Cellular Fixed Relay Networks”, in IEEE VTC 2010 spring, pp.1-5, 2010
- [89] R. Irmer, R. Habendorf, W. Rave and G. Fettweis, “Nonlinear multiuser transmission using multiple antennas for TDD-CDMA,” in Proc. WPMC, vol. 3, pp. 251–255, Oct. 2003
- [90] P.A. Parker et al., “On Bounds and Algorithms for Frequency Synchronization for Collaborative Communication Systems”, in IEEE Transactions on Signal Processing, vol.56, issue 8, part 1, pp.3742-3752, 2008

REFERENCE

- [91] G. Caire and S. Shamai, "On the Achievable Rates of a Multi-antenna Gaussian Broadcast Channel", in proceedings of IEEE International Symposium on Information Theory 2001, pp.147, 2001
- [92] S.K. Jayaweera and H.V. Poor, "On the capacity of multiple-antenna systems in Rician fading", in IEEE Transactions on Wireless Communications, vol.4, issue 3, pp.1102-1111, 2005
- [93] H. Bolckei, D. Gesbert and A.J. Paulraj, "On the Capacity of OFDM-Based Spatial Multiplexing Systems", in IEEE Transactions on Communications, vol.50, issue 2, pp.225-234, 2002
- [94] N. Jindal, S. Vishwanath and A. Goldsmith, "On the duality of Gaussian multiple-access and broadcast channels", in proceedings of IEEE International Symposium on Information Theory 2002, pp.500, 2002
- [95] T. Riihonen et al., "On the feasibility of full-duplex relaying in the presence of loop interference", in IEEE 10th Workshop on SPAWC'09, pp.275-279, 2009
- [96] H. Wu, T. Haustein, and P. A. Hoeher, "On the information rate of single-carrier FDMA using linear frequency domain equalization and its application for 3GPP-LTE uplink," EURASIP Journal on Wireless Communications and Networking, vol. 2009, 2009.
- [97] K. Karakayali et al., "On the maximum common rate achievable in a coordinated network", in IEEE ICC'06, pp.4333-4338, 2006
- [98] E. Zimmermann, P. Herhold, and G. Fettweis, "On the performance of cooperative relaying protocols in wireless networks," European Transactions on Telecommunications, vol. 16, no. 1, pp. 5-16, 2005
- [99] David Martín-Sacristán et al., "On the way towards fourth-generation mobile: 3GPP LTE and LTE-advanced", in EURASIP Journal on Wireless Communications and Networking, 2009, p.1-10, March 2009
- [100] S. Fang, G. Wu and S. Li, "Optimal Multiuser MIMO Linear Pre-coding with LMMSE Receiver", in EURASIP Journal on Wireless Communications and Networking, 2009, March 2009
- [101] T. Riihonen, S. Werner and R. Wichman, "Optimized Gain Control for Single-Frequency Relaying with Loop Interference", in IEEE Transactions on Wireless Communications, vol.8, issue 6, pp.2801-2806, 2009
- [102] S. Nagata et al., "Optimum Resource Block Bandwidth for Frequency Domain Channel-Dependent Scheduling in Evolved UTRA Downlink OFDM Radio Access", in IEEE VTC 2006 spring, pp.206-210, 2006

- [103] Y. Zhu, Y. Xin and PY Kam, "Outage Probability of Rician Fading Relay Channels", in IEEE MILCOM 2006, pp.1-6, 2006
- [104] J.G. Andrews, W. Choi and R.W. Heath, "Overcoming Interference in Spatial Multiplexing MIMO Cellular Networks", in IEEE Wireless Communications, vol.14, issue 6, pp.95-104, 2007
- [105] A. Bou Saleh et al., "Performance of Amplify-and-Forward and Decode-and-Forward Relays in LTE-Advanced", in IEEE VTC 2009 fall, pp.1-5, 2009
- [106] Z. Zeng, "Performance of the Frequency Domain Packet Scheduling for LTE Downlink", in ICICC 2010, vol.1, pp.635-638, 2010
- [107] T. Khoa et al., "Power Allocation and Admission Control in Multiuser Relay Networks via Convex Programming, Centralized and Distributed Schemes", in EURASIP Journal on Wireless Communication And Networking, vol. 2009, 2009
- [108] M. Salem et al., "Radio Resource Management in OFDMA-based Cellular Networks Enhanced with Fixed and Nomadic Relays", in IEEE WCNC 2010, pp.1-6, 2010
- [109] W. Steven et al., "Relay Architectures for 3GPP LTE-Advanced", in EURASIP Journal on Wireless Communication And Networking, vol. 2009, 2009
- [110] B. Niu et al., "Relay Assisted Cooperative OSTBC Communication with SNR Imbalance and Channel Estimation Errors", in IEEE VTC 2009 spring, pp.1-5, 2009
- [111] R. Pabst et al., "Relay-Based Deployment Concepts for Wireless and Mobile Broadband Radio", in IEEE Communications Magazine, vol.42, issue 9, pp.80-89, 2004
- [112] A.D. Wyner, "Shannon-theoretic approach to a Gaussian cellular multiple-access channel", in IEEE Transactions on Information Theory, vol.40, issue 6, pp.1713-1727, 1994
- [113] P. Viswanath and D.N.C. Tse, "Sum capacity of the vector Gaussian broadcast channel and uplink-downlink duality", in IEEE Transactions on Information Theory, vol.49, issue 8, pp.1912-1921, 2003
- [114] H. Ekstrom et al., "Technical solutions for the 3G long-term evolution", in IEEE Communications Magazine, vol.44, issue 3, pp.38-45, 2006
- [115] H. Weingarten, Y. Steinberg and S. Shamai, "The Capacity Region of the Gaussian Multiple-Input Multiple-Output Broadcast Channel", in IEEE Transactions on Information Theory, vol.52, issue 9, pp.3936-3964, 2006
- [116] S. Parkvall, E. Dahlman, A. Furuskar, et al., "LTE-advanced--evolving LTE towards

REFERENCE

- IMT-advanced," in Proceedings of the IEEE Vehicular Technology Conference (VTC '08), pp. 1-5, September 2008.
- [117] O. Simeone et al., "Throughput of low-power cellular networks with collaborative base station and relaying", in IEEE Transactions on Information Theory, vol.54, issue 1, pp.459-467, 2008
- [118] R. A. Horn, C. R. Johnson, "Topics in Matrix Analysis", Cambridge University Press, 1991.
- [119] C.T.K. Ng and A.J. Goldsmith, "Transmitter Cooperation in Ad-Hoc Wireless Networks: Does Dirty-Paper Coding Beat Relaying?", in IEEE ITW 2004, pp.277-282, 2004
- [120] B. Suard et al., "Uplink channel capacity of space-division-multiple-access schemes", in IEEE Transactions on Information Theory, vol.44, issue 4, pp.1468-1476, 2002
- [121] O. Simeone et al., "Uplink Throughput of TDMA Cellular networks with Multicell Processing and Amplify-and-Forward Cooperation Between Mobiles", in IEEE Transactions on Wireless Communications, vol.6, issue 8, pp.2942-2951, 2007
- [122] Wei Yu, "Uplink-downlink duality via minimax duality", in IEEE Transactions on Information Theory, vol.52, issue 2, pp.361-374, 2006
- [123] Christian Siegl and Robert F.H. Fischer. Uplink-downlink duality with regard to constraints imposed in practice. International Journal of Electronics and Communications, July 2009
- [124] WINNER II D1.1.2 V1.0, "WINNER II Channel Models", Sept 2007, <http://www.ist-winner.org/WINNER2-Deliverables/D1.1.2.zip>
- [125] A. Goldsmith, "Wireless Communications", Cambridge, U.K. Cambridge University Press, 2005
- [126] Q.H. Spencer, A.L. Swindlehurst and M. Haardt, "Zero-forcing methods for downlink spatial multiplexing in multiuser MIMO channels", in IEEE Transactions on Signal Processing, vol.52, issue 2, pp.461-471, 2004
- [127] A. Lo and P. Guan, "Performance of In-band Full-Duplex Amplify-and-Forward and Decode-and-Forward Relays with Spatial Diversity for Next-Generation Wireless Broadband", in proceedings of 25th International Conference on Information Networking, 2011
- [128] A. Lo, and I. Niemegeers, "Multi-hop Relay Architectures for 3GPP LTE-Advanced", in proceedings of the 2009 IEEE 9th Malaysia International Conference on Communications, pp 15 -17, December 2009, Kuala Lumpur, Malaysia
- [129] A. Lo and P. Guan, "Joint cooperative shared relaying and multipoint coordination for network MIMO in LTE-Advanced Multihop cellular network", book chapter, to appear in "Mobile

Telecommunication”, 2011

List of Figures

Figure 1.1.Capacity versus SNR for different antenna configurations: $M = 1, 2, 4$ and 8	2
Figure 1.2.Illustrations of inter-cell interference: downlink (left) and uplink (right)	3
Figure 2.1.LTE-Advanced Multi-hop Cellular Network Architecture [128].....	7
Figure 2.2.MIMO BC (left) and MIMO MAC (right)	13
Figure 3.1.The relay channel.....	15
Figure 3.2.Loop Interference cancelling	17
Figure 3.3.Half duplex relaying: transmissions in time slot $[i]$ (above) and time slot $[i + 1]$ (below) ..	19
Figure 3.4.Full-duplex relaying	22
Figure 3.5.Capacity versus receive SNR of Relay Link: HDX AF, FDX AF, HDX DF and FDX DF .	25
Figure 3.6.Capacity versus receive SNR of Access Link: HDX AF, FDX AF, HDX DF and FDX DF	26
Figure 3.7.Downlink transmissions in a relay network with a 2-antenna UE.....	27
Figure 3.8.Capacities of 1- and 2-antenna UEs versus P	28
Figure 3.9.Outage probabilities (at $R=2\text{bps/Hz}$) of 1- and 2-antenna UEs versus P	29
Figure 4.1.The pre-coding process in base station coordination.....	32
Figure 4.2.Uplink (above) and downlink (below) transmissions in a conventional network.....	35
Figure 4.3.Uplink (above) and downlink (below) transmissions with base station coordination	37
Figure 4.4.Downlink sum-rate capacity versus P_{eNB} : conventional and base station coordination	40
Figure 4.5.Uplink sum-rate capacity versus P_{UE} : conventional and base station coordination.....	41
Figure 4.6.Downlink outage probability (at $R=2\text{bps/Hz}$) versus P_{eNB} : conventional and base station coordination	42
Figure 4.7.Uplink outage probability (at $R=1\text{bps/Hz}$) versus P_{UE} : conventional and base station coordination	43
Figure 4.8.Downlink sum-rate capacity versus P_{eNB} : theoretical and zero-forcing base station coordination	44
Figure 4.9.Downlink outage probability (at $R=2\text{bps/Hz}$) versus P_{eNB} : theoretical and zero-forcing base station coordination.....	45
Figure 5.1.Uplink (above) and downlink (below) transmissions with shared relaying.....	47
Figure 5.2.Uplink (above) and downlink (below) transmissions in the combination scheme	49
Figure 5.3.Downlink sum-rate capacity versus P_{eNB} : four Scenarios	54
Figure 5.4.Uplink sum-rate capacity versus P_{UE} : four Scenarios.....	55
Figure 5.5.Downlink sum-rate capacity versus P_{UE} : four Scenarios.....	56
Figure 5.6.Uplink sum-rate capacity versus P_{RN} : four Scenarios	57

Figure 5.7. Downlink sum-rate capacity versus distance apart from RN: four scenarios 58
Figure 5.8. Uplink sum-rate capacity versus distance apart from RN: four scenarios 59

List of Tables

Table 1.1.ITU and 3GPP requirements [116]	1
Table 5.1.Simulation parameters	53